

Fig. 2 XRD patterns of PT ceramics singly sintered at various temperatures.

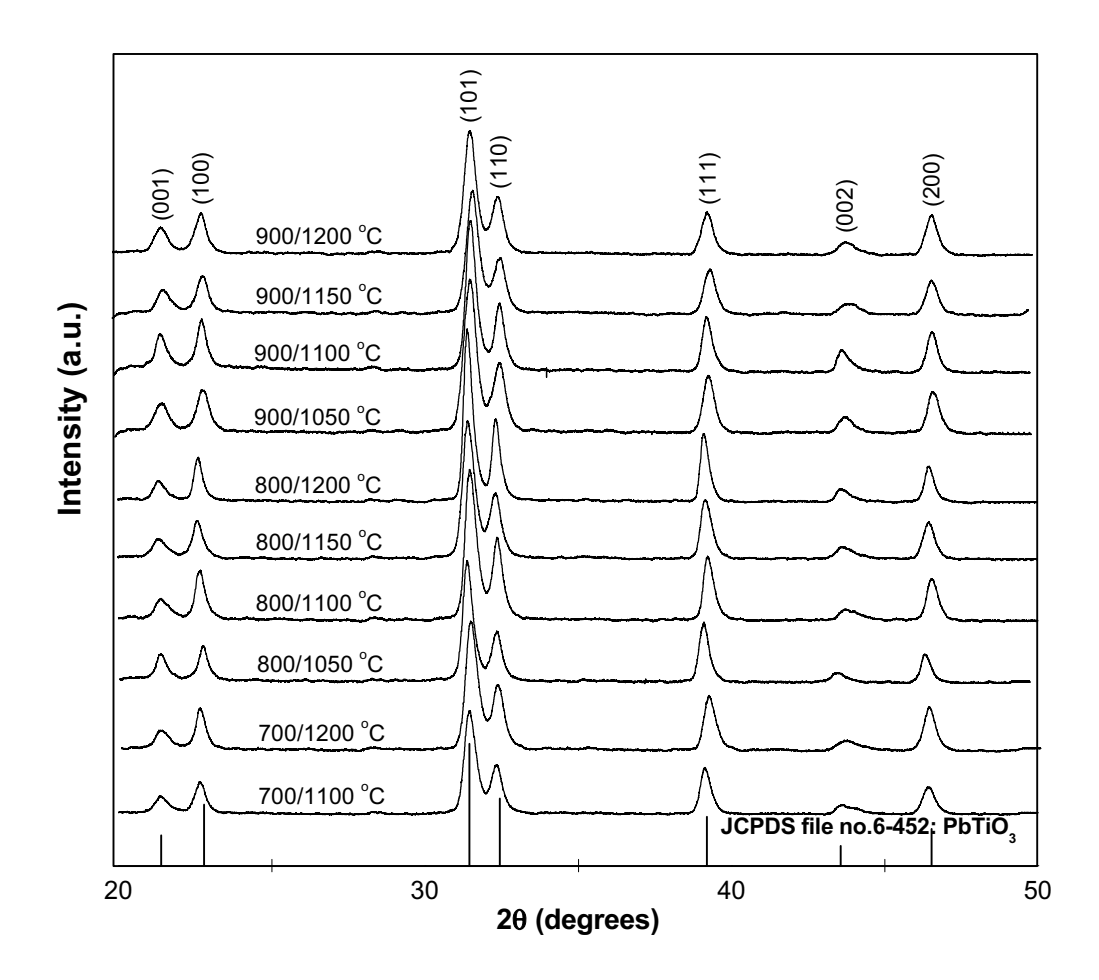


Fig. 3 XRD patterns of PT ceramics doubly sintered at various conditions, with the first sintering temperature (T_1) at 700, 800 and 900 $^{\circ}$ C.

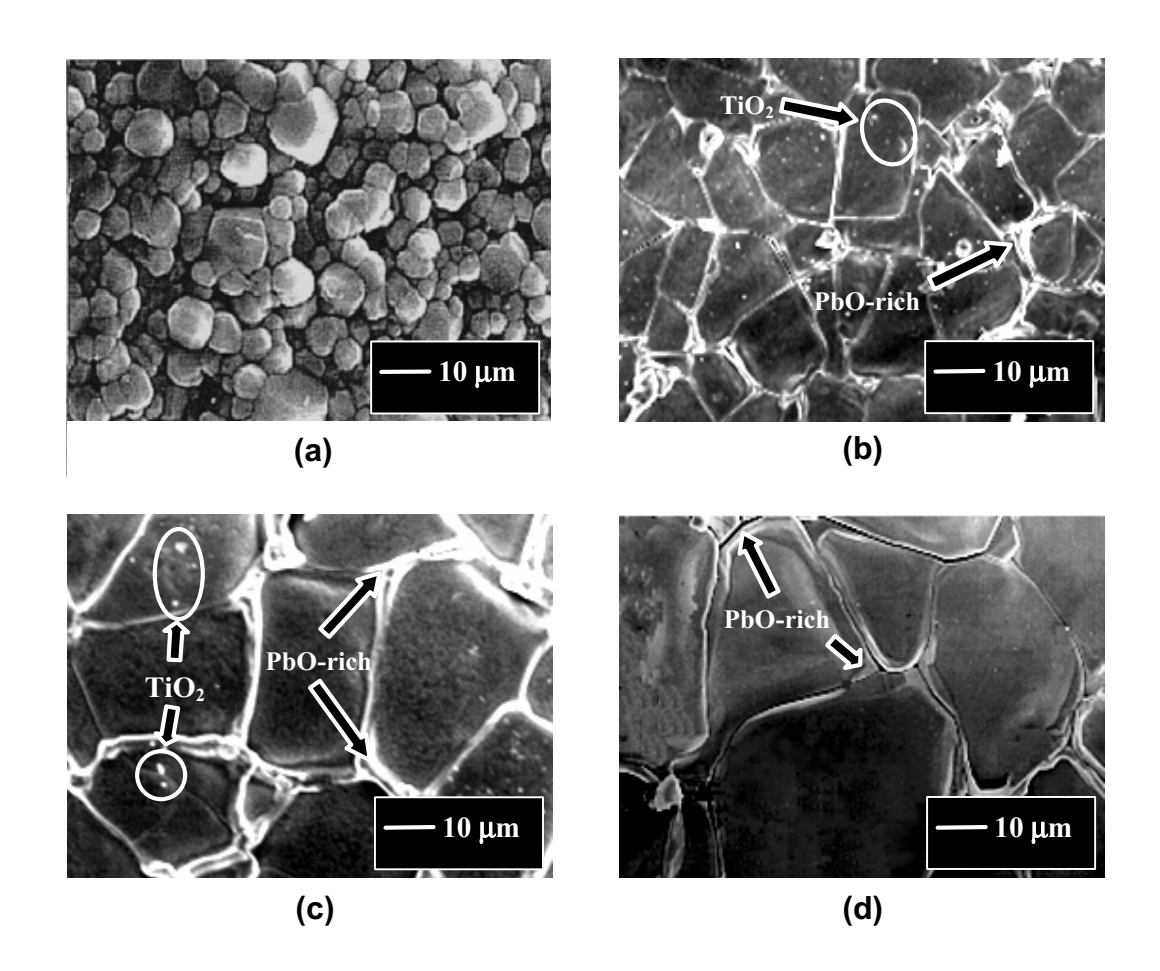


Fig. 4 SEM micrographs of PT ceramics singly sintered at (a) 1150 (b) 1175 (c) 1200 and (d) 1225 $^{\circ}$ C.

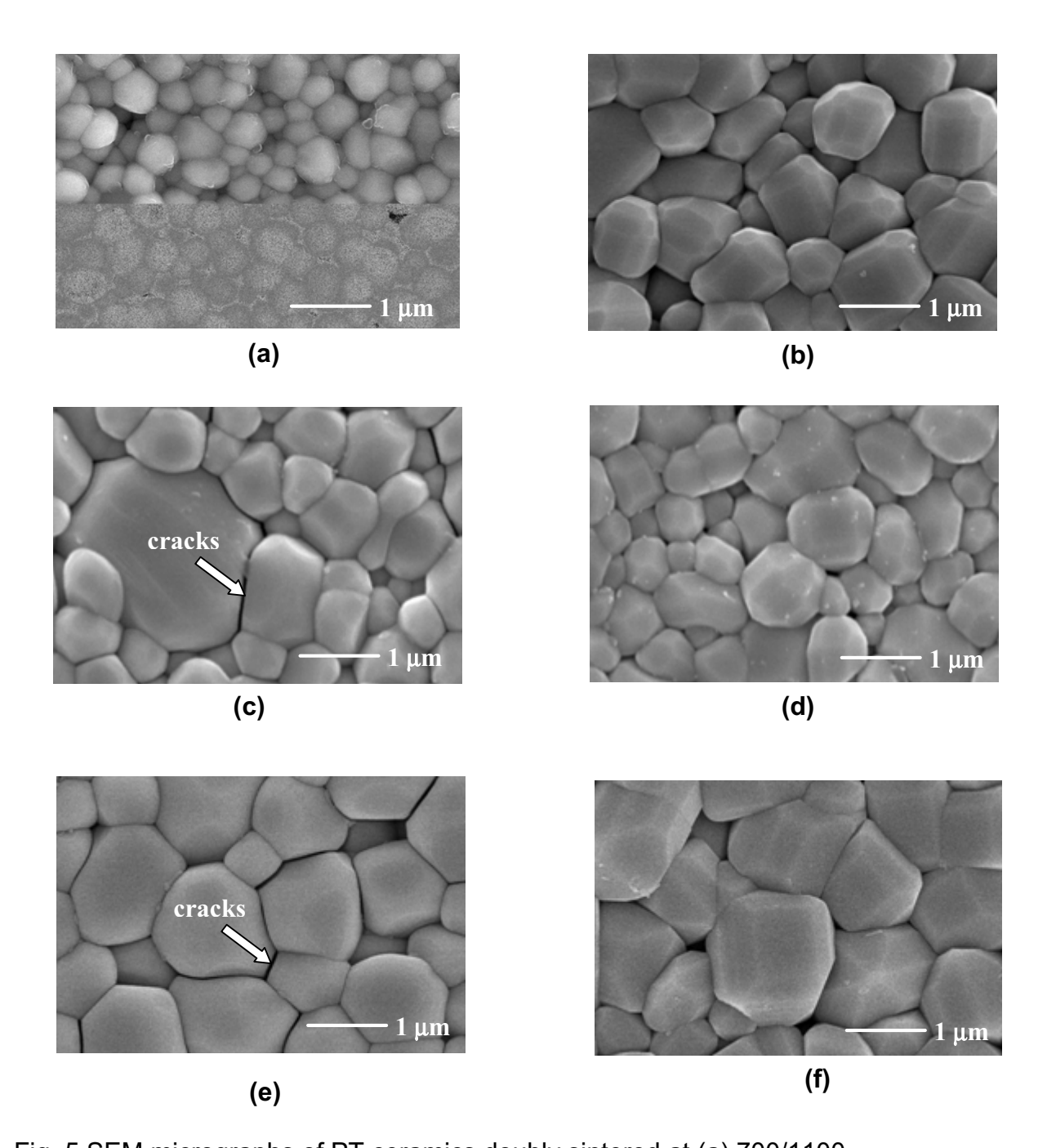


Fig. 5 SEM micrographs of PT ceramics doubly sintered at (a) 700/1100 (b) 700/1200 (c) 800/1100 (d) 800/1200 (e) 900/1100 and (f) 900/1200 $^{\circ}$ C.

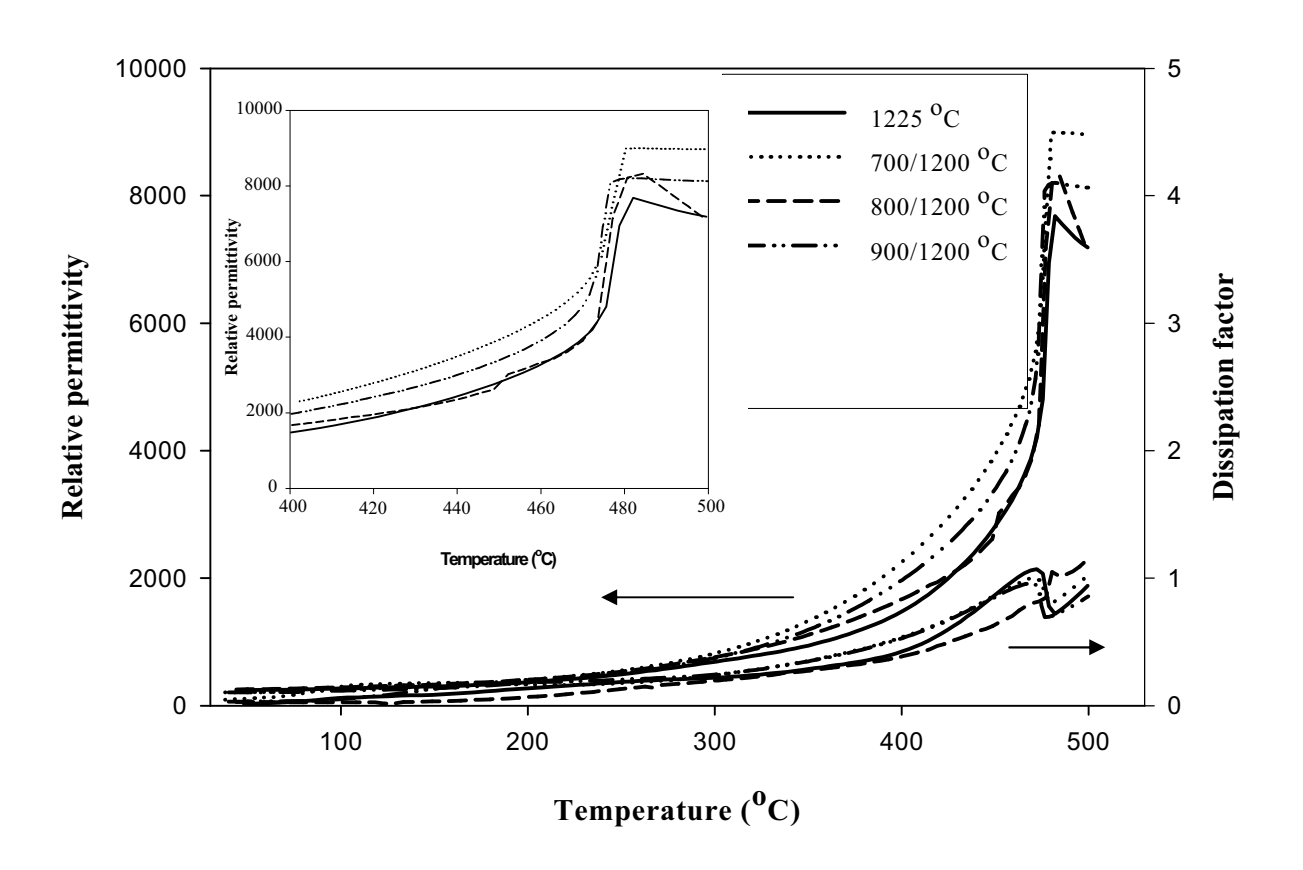


Fig. 6 Variation with temperature of (a) relative permittivity (r) and (b) dissipation factor (tan) at 1 MHz for PT ceramics sintered at various conditions (inset: relative permittivity vs temperature from 400 °C to 500 °C).

The Fabrication of Lead Titanate Ceramics by a Two-Stage Sintering Technique

R. Wongmaneerung*, O. Khamman, R. Yimnirun and S. Ananta

Department of Physics, Faculty of Science, Chiang Mai University,

Chiang Mai, Thailand, 50200 Email: re nok@yahoo.com

Abstract

In this work, a two-stage sintering technique, which began with an initial heating at

lower temperature and followed by higher temperature sintering, was employed in the

production of PbTiO₃ ceramics. Effects of designed sintering conditions on phase formation,

densification, microstructure and dielectric properties of the ceramics were characterized via

X-ray diffraction (XRD), Archimedes method, scanning electron microscopy (SEM) and

dielectric measurement, respectively. The potentiality of a two-stage sintering technique as a

low-cost and simple ceramic fabrication to obtain highly dense and pure lead titanate

ceramics was demonstrated. It has been found that, under suitable conditions, the perovskite

phase of densified PT ceramics with reasonable dielectic properties may be achieved with

equivalent to those obtained from a single-stage sintering technique.

Keyword: Lead titanate; PbTiO₃; Two-Stage Sintering; Perovskite; Microstructure

1

1. Introduction

Lead titanate (PbTiO₃ or PT) when combined with other oxides can form a series of ferroelectric materials that exhibit many of the most desirable dielectric, piezoelectric and pyroelectric properties for high frequency and temperature applications [1-3]. However, pure and dense PT ceramics are regarded to be one of the most difficult lead-based perovskite ferroelectric ceramics to produce due to large distortion of the tetragonal phase at room temperature (c/a, hereafter called tetragonality, ~ 1.06) [4]. Apart from general problems of PbO volatilization and associated high porosity, the stress induced by cooling through the phase transition can create cracking in bulk ceramics.

To overcome these problems, several techniques have been introduced, such as utilizing ultrafine powders, using additives, and carrying out appropriated milling and sintering conditions [5-7]. Amongst all the issues reported so far, most attention has been concentrated on the use of additives and powder processing, whereas investigations on modified sintering techniques have not been widely carried out [8]. Therefore, in the present study, a two-stage sintering method has been developed to resolve these problems. The overall aim of the work described here is to design the sintering scheme for fabrication of PT ceramics. The effect of the sintering conditions on phase formation, densification, microstructure and dielectric properties of materials is then investigated.

2. Experimental Procedure

Commercially available powders of PbO and TiO₂ (anatase form) (Fluka, > 99% purity) were used as starting materials. A simple mixed oxide synthetic route reported earlier [7] was employed to synthesize PbTiO₃ powders. Ceramic fabrication was carried out by adding 3 wt% polyvinyl alcohol (PVA) binder, prior to pressing as pellets in a uniaxial die

press at 100 MPa. Sintering was carried out with a dwell time of 2 h for each step, with constant heating/cooling rates of 1 °C/min. Variation of the single sintering temperature between 1150 and 1250 °C was carried out for the first batch of the samples. For the second batch, the first sintering temperature (T₁) was assigned at 900 °C for all cases. Variation of the second sintering temperature (T₂) from 1000 °C to 1250 °C was carried out.

Densities of the sintered products were determined by using the Archimedes principle. Sintered ceramics were examined by room temperature X-ray diffraction (XRD; Siemens-D500 diffractometer) to identify the phase formed. The lattice parameters were calculated from the XRD patterns. The microstructural development was characterized using a JEOL JSM-840A scanning electron microscopy (SEM) equipped with an energy dispersive X-ray (EDX) analyzer. Mean grain sizes of the sintered ceramics were estimated by employing the linear intercept method. The dielectric properties were measured using a HIOKI 3532-50 LCR meter.

3. Results and Discussion

X-ray diffraction patterns from the singly and doubly sintered PT ceramics are displayed in Figs. 1 and 2, respectively, indicating the formation of both perovskite and impurity phases in each case. The strongest reflections in the majority of the XRD traces indicate the formation of the perovskite phase of lead titanate, PbTiO₃, which could be matched with JCPDS file no. 6-452, in agreement with other works [5,7,9]. For the singly sintered PT ceramics, additional weak reflections are found in the samples sintered above 1175 °C (marked by ▼ in Fig. 1), which correlate to the starting precursor PbO (JCPDS file no.77-1971). This observation could be attributed mainly to the poor mixing of the employed powders derived from the ball-milling technique. More interestingly, a single phase of perovskite is found in most of the doubly sintered PT samples (Fig. 2), in contrast to the

observations for the singly sintered samples. This could be due to the lower firing temperature of the doubly sintered samples as compared to the singly sintered ceramics, leading to a smaller degree of lead losses and consequently avoiding the pyrochlore formation. However, many other factors come into play, e.g. homogeneity of materials, reactivity of starting powders, and processing variables.

From Table 1, it is evident that as the sintering temperature increases, the density of almost all the samples increases. The ceramic doubly sintered at 900/1150 °C having the highest relative density of about 98% with a smallest average grain size of about 0.8 m, was of the best interest for further investigations. Nevertheless, most of the samples suffered from severe stresses as a result of the high c/a ratio so they have broken into pieces once subjected to a cycle of high temperature measurement of dielectric properties.

Microstructural features of PT samples singly sintered at different temperatures are shown in Fig. 3. It was found that the samples subjected to low sintering temperature e.g. $1150\,^{\circ}$ C eventually burst into pieces because of the internal anisotropic stress caused by the phase transition in the ceramics as can be confirmed by the SEM images showing a loose formation of large grains (Fig. 3(a) and (b)), in consistent with high values of c/a given in Table 1. Additionally, average grain sizes were found to increase with the sintering temperature. For higher temperature treatments, a pronounced second phase is segregated at the grain boundaries. The EDX spectra indicated that there was more Pb and less Ti in the bright region than in the dark region. The observation of these second phase layers could be attributed to a liquid phase formation during the sintering process as proposed by Wang *et al.* and Gupta *et al.* [10,11]. It should also be noted here that the second phase could also be a result of the purity of the commercial grade starting materials and firing history used in this study. In addition, a combination of SEM and EDX techniques has demonstrated that small amounts of nano-sized ($\sim 1.7-2.5$ m) spherical of TiO₂ inclusions (brighter phase) exits on

the surface of perovskite PT grains in some samples, as shown in Fig. 3(b) and (c). The existence of a discrete TiO₂ phase points to the expected problem of poor homogeneity of the samples arised from PbO volatilization after subjected to prolong heating scheme, although the concentration is too low for XRD detection.

Representative microstructures for doubly sintered PT ceramics are given in Fig. 4. It is seen that a uniform grain shape of typical perovskite ceramics [12] is observed, with sizes in the range of 0.4-2.0 m. It should be noted that the average grain size of the doubly sintered PT ceramics is < 1.5 m, which is less than the critical value of 3 m [13] and gives rise to a volumetric percentage enough to buffer the anisotropic stress caused by the phase transition [5]. Here, it is believed that smaller grains with random orientations result in lower internal stress in sintered samples because they compensate the anisotropy of thermal expansion coefficients.

By comparison with singly sintered PT ceramics, almost clean microstructures with highly uniform, denser angular grain-packing are generally found in doubly sintered PT samples. These microstructures are typical of a solid-state sintering mechanism. However, it should be noted that higher angulary grains were evidenced for higher second sintering temperature. The observation that the sintering temperature effect may also play an important role in obtaining a high angularity grains of perovskite ceramics is also consistent with other similar systems [14]. It is also of interest to point out that evidence has been found for the existence of microcracks (arrowed) along the grain boundaries of the samples sintered at lower second sintering temperatures (Fig. 4(a) and (b)), in consistent with other works [8,15].

Interestingly, only the samples sintered at 900 °C/1150 °C with the highest relative density and smallest average grain size of about 98% and 0.8 m, respectively, remained unbroken. It may be assumed that the ceramics consisting of very fine grains suffer less deformation, caused by the high value of c/a ratio, than the ceramics with significantly large

grains (Table 1). Consequently, the experimental work carried out here suggests that the optimum conditions for forming the highly dense PT ceramics in this work are double-sintering temperatures at 900 °C/1150 °C, 2 h dwell time, and 1 °C/min heating/cooling rates. The dielectric properties of PT samples sintered with different techniques are also compared in Table 2. In general, they all behave as normal ferroelectric. The Curie temperatures are about the same for all samples measured whilst the variation of dielectric constant and dielectric loss of both sets of the sintered PT ceramics seems to be somewhat related to the sintering temperatures. This observation indicates that the presence of the second phases accompanied with porosities is the key factor responsible for the dielectric response of the products. Moreover, this study demonstrated that the dielectric properties of PT ceramics are also influenced by microstructural features especially the grain boundary phase, microcracks and densification mechanism rather than by only pyrochlore phase or by grain size itself.

4. Conclusion

This work demonstrated that it was possible to obtain rather dense PT ceramics with homogeneous microstructure by the two-stage sintering technique. It has been shown that, under suitable conditions, the phase formation and densification of the ceramics are better than those obtained from the single-stage sintering. More importantly, with the two-stage sintering technique, small reductions in the maximum required sintering temperature are possible as compared to the single-stage sintering.

Acknowledgements

This work was supported by the Thailand Research Fund (TRF), Faculty of Science and Graduate school, Chiang Mai University.

References

- [1]. A.J. Moulson and J.M. Herbert, *Electroceramics*, Wiley, Chichester, 2003.
- [2]. G.H. Haertling, J. Am. Ceram. Soc., 82, 797-818 (1999).
- [3]. S. Jiang, D. Zhou, S. Gong and W. Lu., Sensors Actuat., A69, 1-4 (1998).
- [4]. G. Shirane, R. Pepinsky and B.C. Frazer, Acta Crystallogr., 9, 131-140 (1956).
- [5]. T. Suwannasiri and A. Safari, *J. Am. Ceram. Soc.*, **76**, 3155-3158 (1993).
- [6]. J. Tartaj, C. Moure, L. Lascano and P. Duran, *Mater. Res. Bull.*, 36, 2301-2310 (2001).
- [7]. A. Udomporn, K. Pengpat and S. Ananta, J. Eur. Ceram. Soc., 24, 185-188 (2004).
- [8]. S. Ananta and N.W. Thomas, J. Eur. Ceram. Soc., 19, 2917-2930 (1999).
- [9]. JCPDS-ICDD Card no. 6-452. International Centre for Difraction Data. Newtown Square, PA, 2000.
- [10]. H.C. Wang and W.A. Schulze, J. Am. Ceram. Soc., 73, 825-832 (1990).
- [11]. S.M. Gupta and A.R. Kulkarni, *J. Mater. Res.*, **10**, 953-961 (1995).
- [12]. Y.-C. Liou, Mater. Sci. Eng., **B103**, 281-284 (2003).
- [13]. R.W. Rice and R.C. Pohanka, J. Am. Ceram. Soc., 62, 559-563 (1979).
- [14]. S. Ananta and N.W. Thomas, J. Eur. Ceram. Soc., 19, 1873-1881 (1999).
- [15]. S.R. Dhage, Y.B. Khollam, H.S. Potdar, S.B. Deshpande, B.D. Sarwade and D.K. Date, *Mater. Lett.*, 56, 564-570 (2002).

Captions of tables and figures

- **Table 1** Sintering behaviour of PT ceramics.
- **Table 2** Dielectric properties of PT ceramics.
- **Fig. 1** XRD patterns of PT ceramics singly sintered at various temperatures for 2 h with heating/cooling rates of 1 °C/min.
- Fig. 2 XRD patterns of PT ceramics doubly sintered at various second sintering temperatures.
- **Fig. 3** SEM micrographs of PT ceramics singly sintered at (a) 1150 °C (b) 1200 °C (c) 1225 °C and (d) 1250 °C, for 2 h with heating/cooling rates of 1 °C/min.
- **Fig. 4** SEM micrographs of PT ceramics doubly sintered at (a) 900 °C/1050 °C (b) 900 °C/1100 °C (c) 900 °C/1150 °C and (d) 900 °C/1200 °C, for 2 h with heating/cooling rates of 1 °C/min.

T_2	Tetragonality	Relative density	Mean grain size*
(°C)	(c/a)	(%)	(m)
-	1.064	87	10
-	1.064	89	21
-	1.063	92	29
-	1.063	94	36
-	1.063	93	41
1000	-	-	-
	1.060	6	1.2
	1.060	6	1.1
	1.056	7	0.8
	1.061	7	1.5
1250	-	-	-
	(°C) 1000	(°C) (c/a) - 1.064 - 1.063 - 1.063 - 1.063 1.063 1.060 1.060 1.056 1.056	(°C) (c/a) (%) - 1.064 87 - 1.064 89 - 1.063 92 - 1.063 94 - 1.063 93 1000 1.060 6 1.060 6 1.056 7 1.061 7

^{*} The estimated precision of the grain size is $\pm 1\%$

⁻ Data are not available because the samples were too fragile for the measurements.

Dielectric Properties	Sintering Temperature (°C)	
(1 kHz)	1225	900/1200
r, room temperature	525	318
T_{C}	486	487
r, max	20423	416997
tan _{max}	2.35	0.08

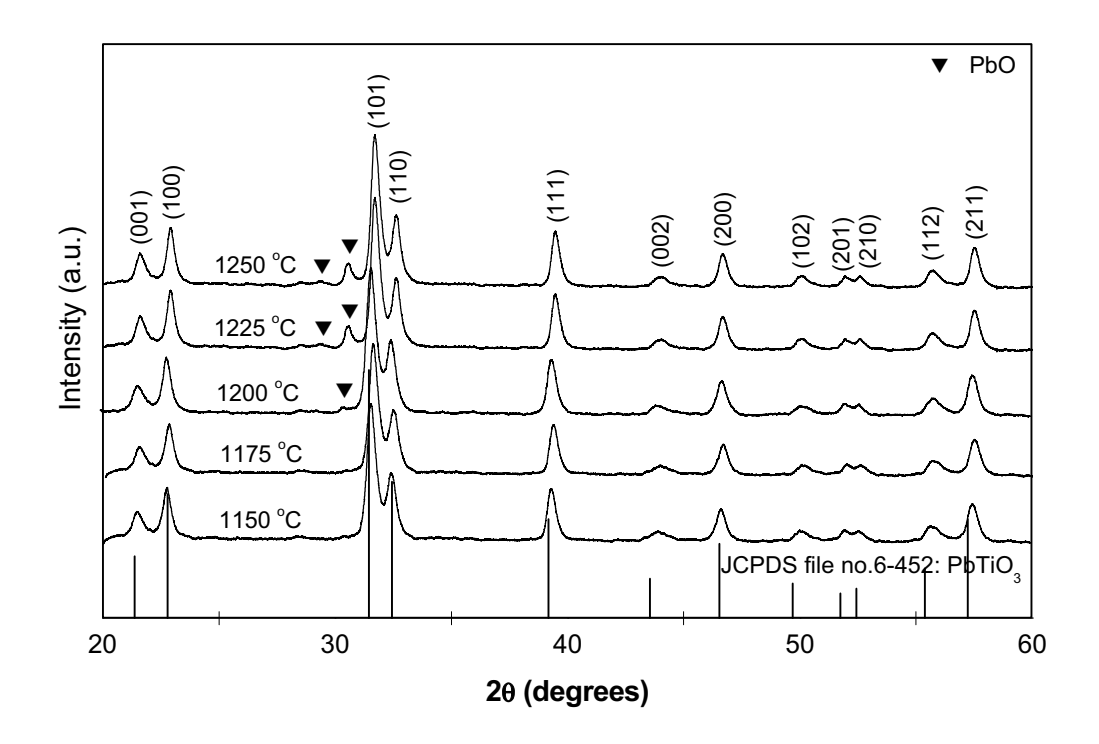


Fig. 1

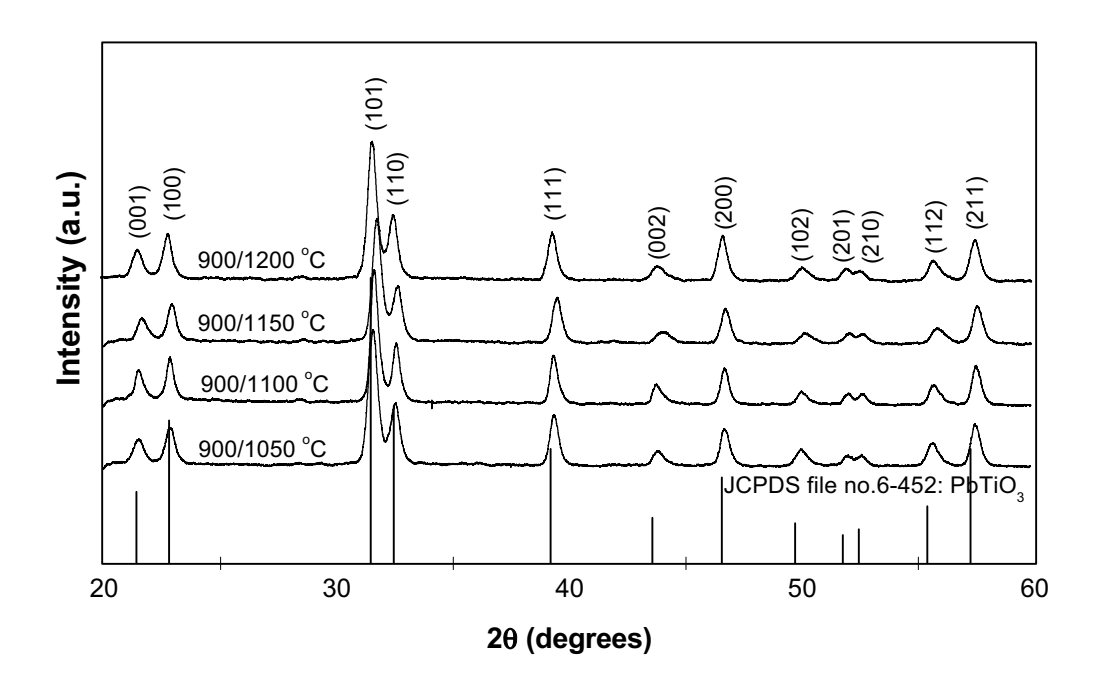


Fig. 2

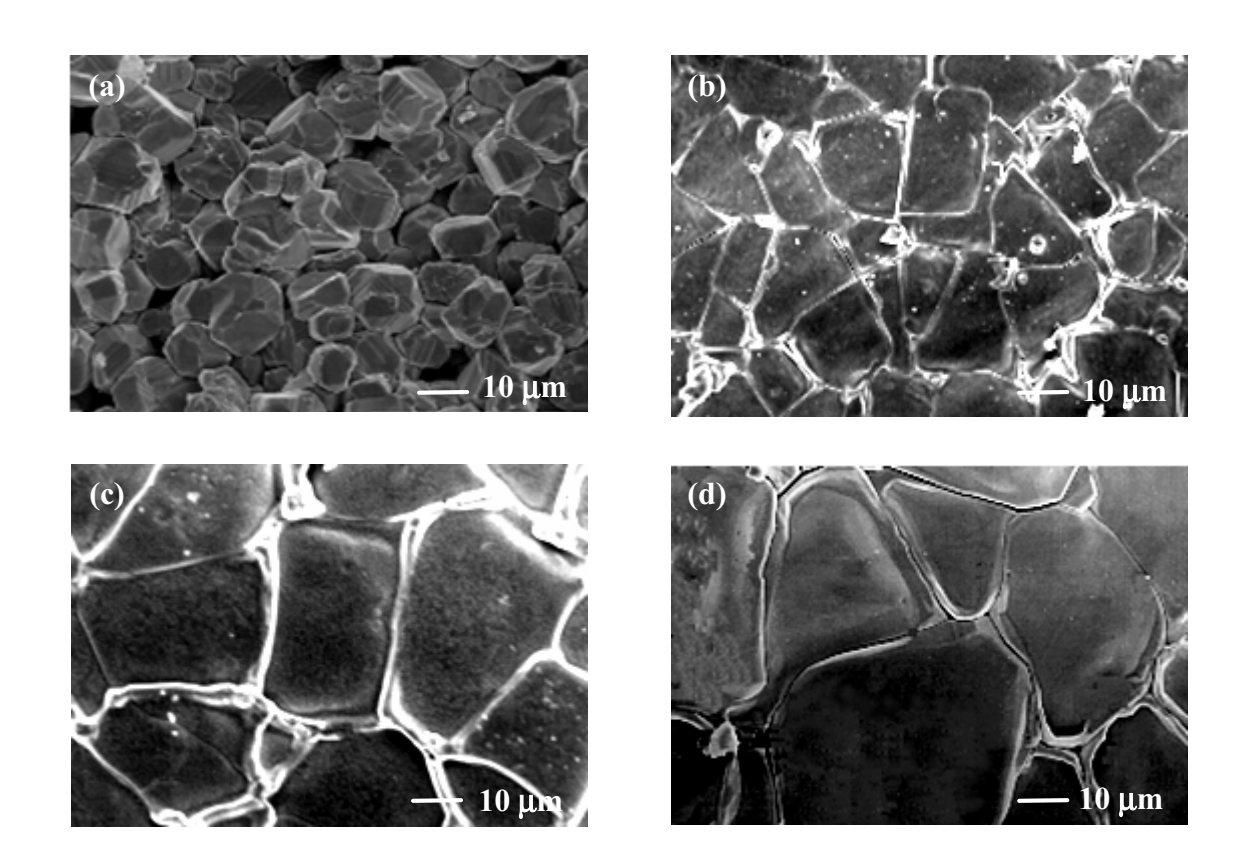


Fig. 3

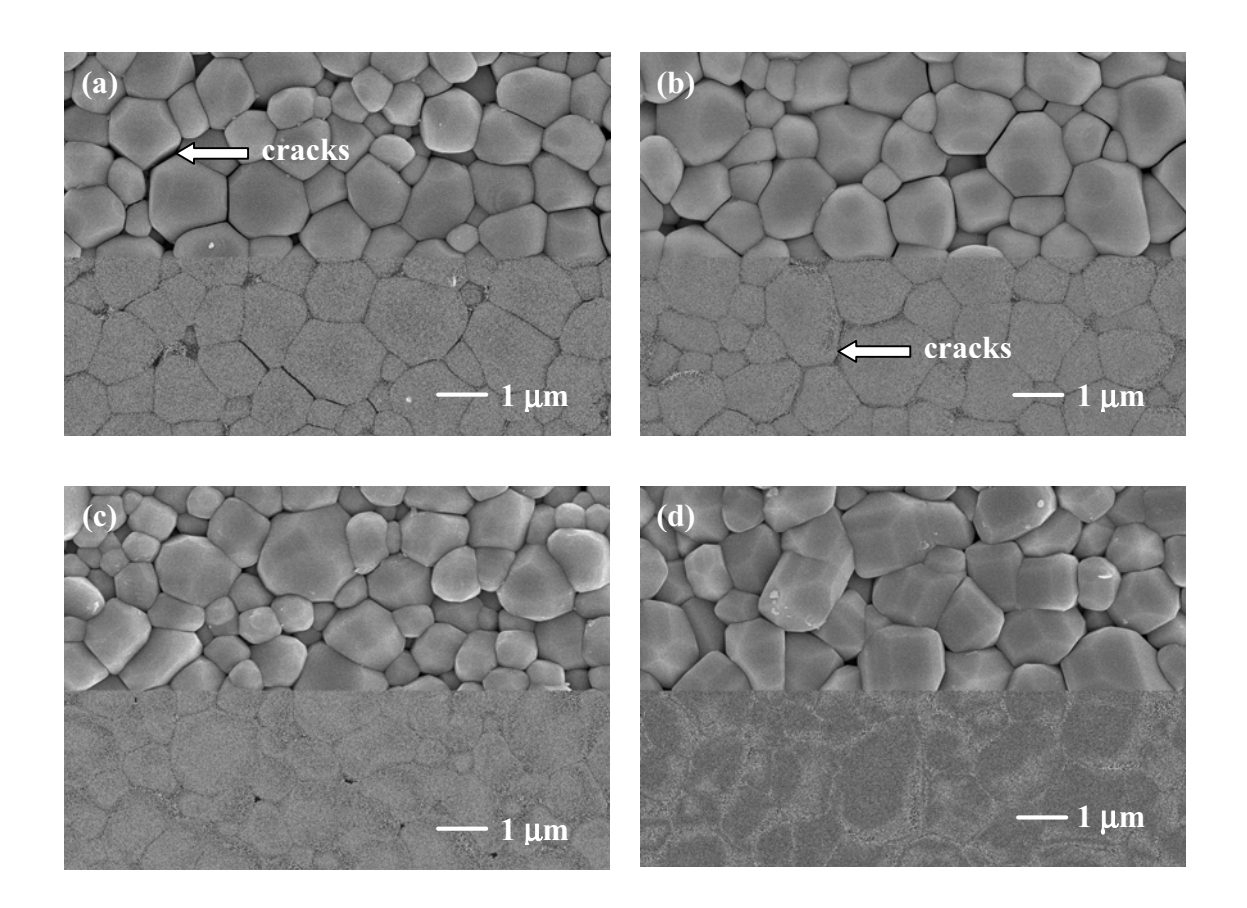


Fig. 4

Scaling Behavior of Dynamic Hysteresis in Soft PZT Bulk

Ceramics

Rattikorn Yimnirun, Yongyut Laosiritaworn, Supattra Wongsaenmai,

and Supon Ananta

Department of Physics, Faculty of Science, Chiang Mai University,

Chiang Mai 50200, Thailand

Corresponding author E-mail: rattikornyimnirun@yahoo.com

PACS numbers: (1) 77.84.Dy (2) 77.80.-e (3) 77.80.Fm

ABSTRACT

The scaling behavior of the dynamic hysteresis of ferroelectric bulk system

was investigated. The most novel point in the study is to report the scaling relation of

the soft PZT bulk ceramic which takes a form of $< A > \infty f^{-1/4} E_0$. The exponent to the

field-amplitude was found to be significantly lower than that of the theoretical

prediction on $(\phi^2)^2$ and $(\phi^2)^3$ models. However, a slower decay of the hysteresis

loop-area with frequency than PZT thin film was found, which states that the scaling

relation is dimensionally dependent, and depolarizing effects in the interior must be

taken into account to model bulk materials.

Key words: Scaling, Hysteresis, Ceramics, soft PZT

1

Lead zirconate titanate (Pb(Zr_{1-x}Ti_x)O₃ or PZT) ceramics have been employed extensively in sensor and actuator applications, as well as smart systems.¹ The most widely studied and used PZT compositions are in the vicinity of the morphotropic phase boundary (MPB) between the tetragonal and rhombohedral ferroelectric phases.^{2,3} However, to meet the requirements for specific applications, PZT ceramics are usually modified with dopants.²⁻⁴ Generally, donor (higher-valency) additives induce "soft" piezoelectric behaviors with higher dielectric and piezoelectric activities suitable for sensor and actuator applications. ¹⁻³ In many of these applications, as well as in more recently developed ferroelectric random access memories (Fe-RAMs), the dynamic hysteresis characteristics have become important consideration.^{5,6} In addition to the domain kinetics studies, 7 the dynamic hysteresis, i.e., hysteresis area < A > as a function of the field amplitude E_0 and frequency f, presents a lot of information critical for many ferroelectric applications whose performance is related to the signal amplitude and frequency. 1,6 Theoretical studies have been carried out to understand the dynamic response of hysteresis curves in spin systems.⁸⁻¹¹ In particular, attention is focused on scaling law $< A > \infty f^{\alpha} E_0^{\beta}$ (where α and β are exponents that depend on the dimensionality and symmetry of the system). The theoretical three-dimensional models $((\Phi^2)^2$ and $(\Phi^2)^3$ with O(N) symmetry $(N\to\infty)$) by Rao et al.⁸ and other investigators^{9,12} proposed two scaling relations applicable to the low-f and high-f limits as follows,

$$< A > \propto f^{1/3} E_0^{2/3}$$
 as $f \to 0$, (1)

$$\langle A \rangle \propto f^{-1} E_0^2 \text{ as } f \to \infty$$
 (2)

Apart from its theoretical importance, since reliable measurement of the hysteresis at ultra-high frequency is still a big challenge, it is technologically helpful to

understand the scaling behavior so that the ultra-high frequency of the hysteresis can be predicted. Hence, there has been a great deal of interest in the scaling behavior of the dynamic hysteresis in ferromagnetic and ferroelectric thin films. ¹⁰⁻¹⁴ However, only few investigations on ferroelectric and antiferroelectric bulk systems have been reported. ^{15,16} On a contrary, bulk ferroelectric materials are useful and widely used in many applications. ⁶ Furthermore, to date, there has been no report on the scaling behavior studies of ferroelectric hysteresis loops of bulk ceramics. Consequently, there comes an objective of this study. In this letter, we present the results on the scaling behavior of the dynamic hysteresis of the ferroelectric bulk ceramic, i.e., soft PZT. It should be noted that some discrepancies between the theoretical predictions and the experimental results have already been reported for ferroelectric thin-film systems. ^{11,14,17-21} For extended two-dimensional system, the theoretical studies have predicted the scaling relation at high-*f* limit as in Eq. (2). The experimental investigation, however, on PZT thin film¹⁹ has resulted in a different relation, i.e.,

$$\langle A \rangle \propto f^{-1/3} E_0^3$$
 as $f \to \infty$. (3)

Additionally, another scaling relation has been obtained for the $SrBi_2Ta_9O_4$ thick film, i.e., 17

$$\langle A \rangle \propto f^{-1/3} E_0^2 \quad \text{as} \quad f \to \infty \quad .$$
 (4)

As can be seen, the dimensionality of the structure e.g. thin film in Ref. 19 and thick film in Ref. 17 has a strong effect on the exponent of the scaling relation in Eqs. (3) and (4). It is therefore of great interest to investigate the form of this scaling relation for bulk systems. As it will be shown in this letter, the scaling behavior of the

dynamic hysteresis of the bulk system such as soft PZT ceramic also takes different form.

The disc-shaped samples of a commercially available soft PZT ceramic (PKI-552, Piezo Kinetics Inc., USA) with diameter of 10 mm and thickness of 1 mm were used in this study. The dynamic hysteresis (P-E) loops were characterized at room temperature (25 °C) by using a computer controlled modified Sawyer-Tower circuit with f covering from 2 to 100 Hz and E_0 from 0 to 18 kV/cm. The details of the system were described elsewhere.²²

Figs. 1(a) and 1(b) show the hysteresis loops at different f but fixed E_0 (18 kV/cm), and at different E_0 but fixed f (100 Hz), respectively. As expected, the dependence of the loop pattern and area A > 0 on f and E is remarkable. From Fig 1(a) where E_0 is fixed, one sees the evolution of the pattern at different f. It is very interesting to observe that as the frequency increases the hysteresis changes from an unsaturated loop with near square shape and rounded at the tips at low frequency (2) Hz) to well saturated loops at higher frequencies. The loop area $\langle A \rangle$, remanent polarization (P_r) , and coercive field (E_c) decrease with an increase of frequency. The observation that the $\langle A \rangle$ decreases with increasing frequency in this high-f region is ascribed to the delayed response of the spin reversal to the varying external field. 11,14 It should also be noted that in earlier works by Liu et al. 18,19 on PZT thin film the dependence of the P-E loop shape on frequency differed from that of the current work. Since the magnitude of the applied field and the range of the frequency used were significantly different, the observed difference could be due to the dependence of the loop shape and size on both the field amplitude and frequency, as well as to the different responses to an external field between thin film and bulk ceramics. Figure 1 (b) shows the dependence of the hysteresis loop on the amplitude of the electric field.

For small fields, the loop does not saturate and appears as an ellipse inclined at an angle to the E axis. An increase in the amplitude of the field E_0 makes the loop larger and increases its angle of inclination. For a given frequency of 100 Hz, as shown in Fig. 1(b), loop area A, remanent polarization P_r , and coercive field E_c increase with an increase of E_0 until well saturated loop is achieved.

To investigate the scaling behavior, we followed the previous theoretical predictions on the loop-area^{8,9,12} by plotting the data of <A> against $f^{-1}E_0^2$. This bases on an assumption that Eq. (2) is applicable, and the frequency range used in this study can be considered as the high frequency region in the theoretical predictions since the loop-area decreases with increasing frequencies. The data are shown in Fig. 2(a) and the dotted line represents a fitting in terms of <A> \propto $f^{-1}E_0^2$. Clearly, the theoretically proposed scaling relation in Eq. (2) cannot be directly applied to the data obtained in this study.

On the other hand, earlier experimental work by Liu *et al.*¹⁹ on the scaling behavior of PZT thin film also showed different relation. In those studies, the scaling takes the form of $< A > \infty f^{-1/3} E_0^3$. To check the validity of the relation on the bulk system, i.e., soft PZT ceramic, we plot the data of < A > against $f^{-1/3} E_0^3$. The data are shown in Fig. 2(b) and the dotted line represents a fitting in terms of $< A > \infty f^{-1/3} E_0^3$. Large deviation is also observed in this case. Therefore, this implies that the experimentally obtained scaling relation for the reduced structure i.e. thin film is not applicable to the bulk ceramics.

It is clearly seen that the scaling relations from both the theoretical prediction and the experimental investigation are not applicable for the soft PZT ceramic in this present study. To obtain the suitable scaling relation, one can fit the data with $< A > \propto f^m E_0^n$ where m and n are exponents to be determined directly from the experimental data. By plotting < A > against f at fixed E_0 , one obtains the exponent m. On the other hand, the exponent n can be obtained from plotting < A > against E_0 at fixed f. As plotted in Fig. 3, it is revealed that the data can be much better fitted (with $R^2 = 0.97$), within the measured uncertainty, by

$$\langle A \rangle \propto f^{-1/4} E_0 \tag{5}$$

It should also be noted that there is more deviation from the minor loops without saturation at small field amplitudes, and these data were excluded from the fitting reported. The scaling relation obtained indicates that area A decays more slowly with f and grows more slowly with f than the theoretical prediction, Eq. (2). It is also interesting to see that the area A also decays slightly slower with f, but grows much more slowly with f than the PZT thin film, Eq. (3). There have also been reports on the scaling studies on other bulk systems, such as ferroelectric single crystals f and antiferroelectric bulk system f with very different scaling relations as compared to that of this current study on bulk ceramic. Though these are bulk systems, these are still different types of materials, as compared to the ceramic studied here, thus their scaling behaviors cannot be directly compared.

An explanation for the difference may come from the spin-interaction terms as considered in the $(\Phi^2)^2$ and $(\Phi^2)^3$ models, in which the spin-flip just has one contribution, i.e. spin-reversal.^{8,9} This requires overcoming high energy barrier. Potts model used by Liu *et al.*¹⁹ also has the spin orientation in various domains in directions not anti-parallel to the direction of E, hence requires lower energy barrier for spin-flip to occur, which results in a higher exponent of 3 in the E_0 term, as compared to the exponent of 2 in the theoretical models. However, in ceramics, there

are influences of many depolarizing effects, arisen from domain walls, grain boundaries, space charges, immobile defects etc., which may retard the external field. Consequently, the energy barrier is very much higher, which leads to slower spin-flip kinetics. Therefore, a low exponent for the E_0 term is expected from the ceramics rather than the $(\Phi^2)^2$, $(\Phi^2)^3$ and Potts models, and thin films. This may be the case, as also reported in Ref. 18, why the decay of the area A with frequency f and field amplitude E_0 is much smaller than those from theoretical prediction i.e. $A > \infty f^{-1/3}E_0$ instead of $A > \infty f^{-1}E_0^2$.

In addition, the f-term shows an exponent of -1/4, smaller in absolute value than that of PZT thin-film (exponent is -1/3). To explain the difference, not only the contribution from the domain switching and ionic-type in thin films, 19 one may need to consider the additional contributions to hysteresis properties from space charges on grain boundaries, induced electric-field from interface layers, 23 immobile defects, 24 etc. Since our system is a bulk-ceramic type; therefore, these depolarizing effects, acting as a buffer to spin-reversal mechanism, will be stronger than those in thin film structure. As a result, the hysteresis area must show a relatively weaker dependence on f than that observed in thin films. More importantly, this study shows the difference in experimentally observed scaling behavior between thin film and bulk ceramics, suggesting the different universality class between them.

Although the qualitative explanation of the differences has been presented, a quantitative approach seems to be needed to include the other contributions, in addition to simple spin-interaction. Interestingly, it is theoretically known that the domain reversal can be explained by the nucleation and growth concept. Interestingly, earlier works 10,11 reported that the domain reversal can be characterized by an effective characteristic time (combining simultaneous contributions from both the new domain

nucleation rate and the domain boundary motion velocity) $\tau' \propto E_0^{-1}$. If one considers that at a given frequency this effective characteristic time represents the response of the domain reversal to the varying external field, and should hence be proportional to the hysteresis area, e.g. $< A > \propto E_0^{-1}$. Therefore, if this domain reversal term is combined with the theoretical term which considers only a pure spin-flip mechanism $< A > \propto E_0^2$, one would see the relation $< A > \propto E_0$, which is in good agreement with the current study. This clearly shows that there is still space for improvement in theoretical models.

In summary, we have studied the scaling behavior of the dynamic hysteresis of ferroelectric bulk system, i.e., soft PZT ceramic. The scaling relation of the soft PZT ceramic takes the form of $< A > \propto f^{-1/4} E_0$, which differs significantly from that of the theoretical prediction^{8,9,19} and that of the PZT thin film¹⁸. The differences are attributed to additional contributions from depolarizing effects within the ceramics, as compared to more physically simple structure in thin film, and to simple spin-interaction proposed in the theoretical models. This study clearly serves as a survey to show that more improvement of the theoretical approach is needed to predict the scaling behavior in bulk ceramics.

Financial supports from the Commission on Higher Education (Thailand),
Thailand Research Fund (TRF), Graduate School and Faculty of Science, Chiang Mai
University are gratefully acknowledged.

References

- ¹K. Uchino, Ferroelectric Devices (Marcel Dekker, New York, 2000).
- ²B. Jaffe, W. R. Cook, and H. Jaffe, *Piezoelectric Ceramics* (Academic Press, New York, 1971).
- ³Y.H. Xu, Ferroelectric Materials and Their Applications (North Holland, Los Angeles, 1991).
- ⁴F. Kulcsar, J. Am. Ceram. Soc. **42**, 49 (1959).
- ⁵J.F. Scott, Ferroelectr. Rev. **1**, 1 (1998).
- ⁶K. Uchino, *Piezoelectric Actuators and Ultrasonic Motors* (Kluwer Academic, Boston, 1997).
- ⁷J.D. Gunton, M. San Miguel, and P.S. Sahmi, in *Phase Transitions and Critical Phenomena*, edited by C. Domb and J.L. Lebowitz (Academic, London, 1983), Vol 8, p. 267.
- ⁸M. Rao, H.R. Krishnamurthy, and R. Pandit, Phys. Rev. B **42**, 856 (1990).
- ⁹M. Acharyya and B.K. Chakrabarti, Phys. Rev. B **52**, 6560 (1995).
- ¹⁰J.-M. Liu, H.L.W. Chan, C.L. Choy, and C.K. Ong, Phys. Rev. B **65**, 014416 (2001).
- ¹¹J.-M. Liu, H.L.W. Chan, C.L. Choy, Y.Y. Zhu, S.N. Zhu, Z.G. Liu, and N.B. Ming, Appl. Phys. Lett. **79**, 236 (2001).
- ¹² M. Rao and R. Pandit, Phys. Rev. B **43**, 3373 (1991).
- ¹³Q. Jiang, H.N. Yang, and G.C. Wang, Phys. Rev. B **52**, 14911 (1995).
- ¹⁴B. Pan, H. Yu, D. Wu, X.H. Zhou, and J.-M. Liu, Appl. Phys. Lett. **83**, 1406 (2003).
- ¹⁵S. Hashimoto, H. Orihara, and Y. Ishibashi, J. Phys. Soc. Jpn. **63**, 1601 (1994).
- ¹⁶Y.-H. Kim and J.-J. Kim, Phys. Rev. B. **55**, R11933 (1997).
- ¹⁷J.-H. Park, C.-S. Kim, B.-C. Choi, B.K. Moon, J.H. Jeong, and I.W. Kim, Appl. Phys. Lett. **83**, 536 (2003).
- ¹⁸J.-M. Liu, H.P. Li, C.K. Ong, and L.C. Lim, J. Appl. Phys. **86**, 5198 (1999).
- ¹⁹J.-M. Liu, H.L.W. Chan, and C.L. Choy, Mater. Lett. **52**, 213 (2002).
- ²⁰J.-M Liu, B. Pan, K.F. Wang, and H. Yu, Ceram. Inter. **30**, 1471 (2004)
- ²¹ J.-M. Liu, H. Yu, B. Pan, and X.Y. Chen, Mater. Sci. Eng. **B118**, 2 (2005).
- ²²R. Yimnirun, Y. Laosiritaworn, and S. Wongsaenmai, J. Phys. D: Appl. Phys. **39**, 759 (2006).
- ²³D. Bolten, U. Böttger, and R. Waser, Appl. Phys. Lett. **84**, 2379 (2004).
- ²⁴D. Bolten, U. Böttger, and R. Waser, Jpn. J. Appl. Phys. **41**, 7202 (2002).

List of Figure Captions

- **Fig. 1** Hysteresis loops for soft PZT ceramic (a) at various f and $E_0 = 18$ kV/cm and (b) at various E_0 and f = 100 Hz.
- **Fig. 2** Scaling of hysteresis area <A> against (a) $f^{-1}E_0^2$ and (b) $f^{-1/3}E_0^3$ for soft PZT ceramic.
- **Fig. 3** Scaling of hysteresis area <*A*> against $f^{-1/4}E_0$ for soft PZT ceramic.

Fig. 1 (a)

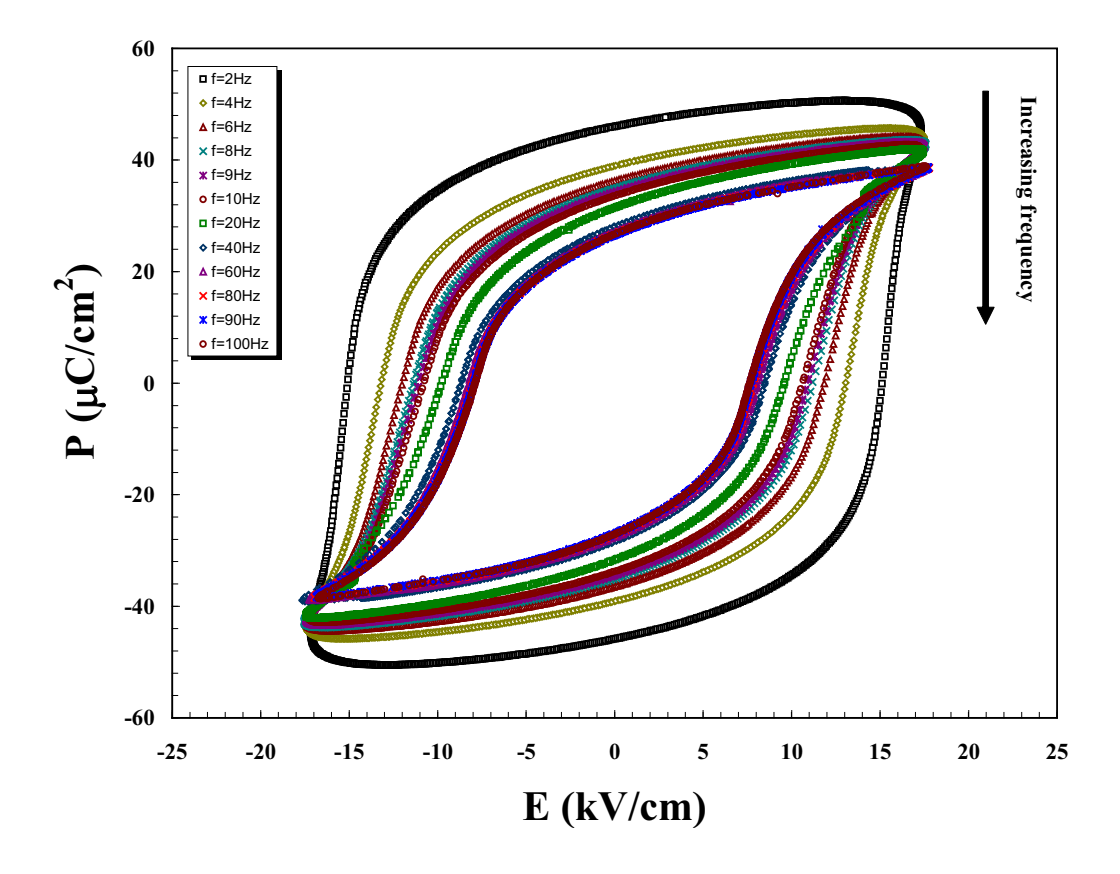


Fig. 1 (b)

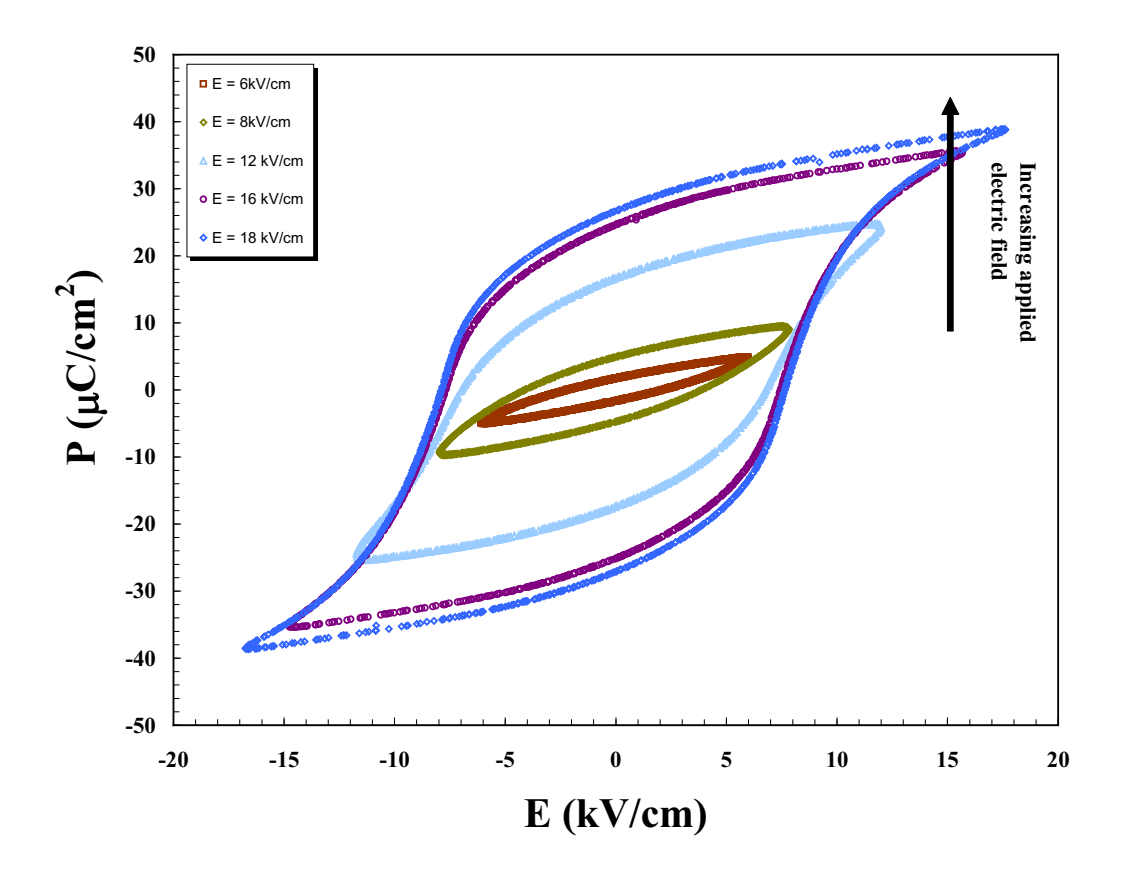


Fig. 2 (a)

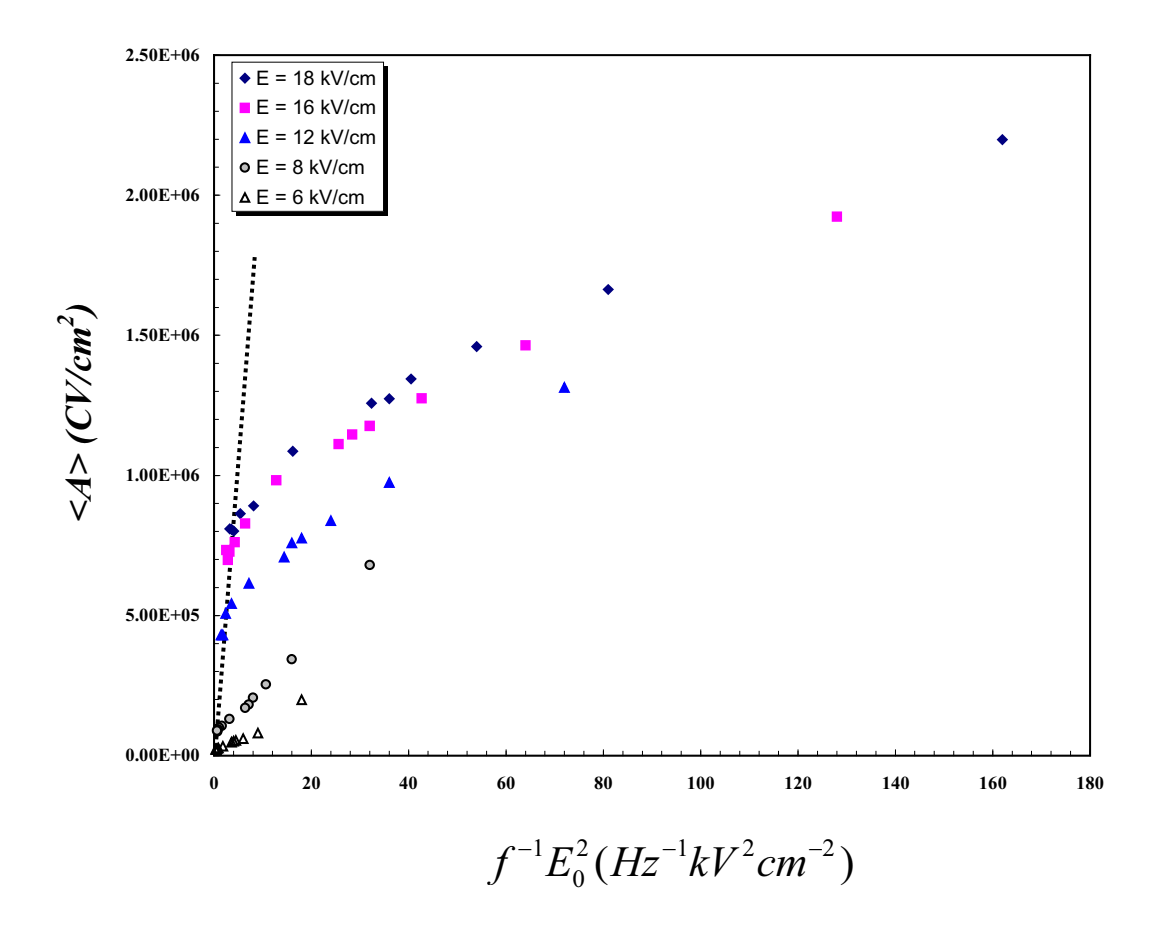


Fig. 2 (b)

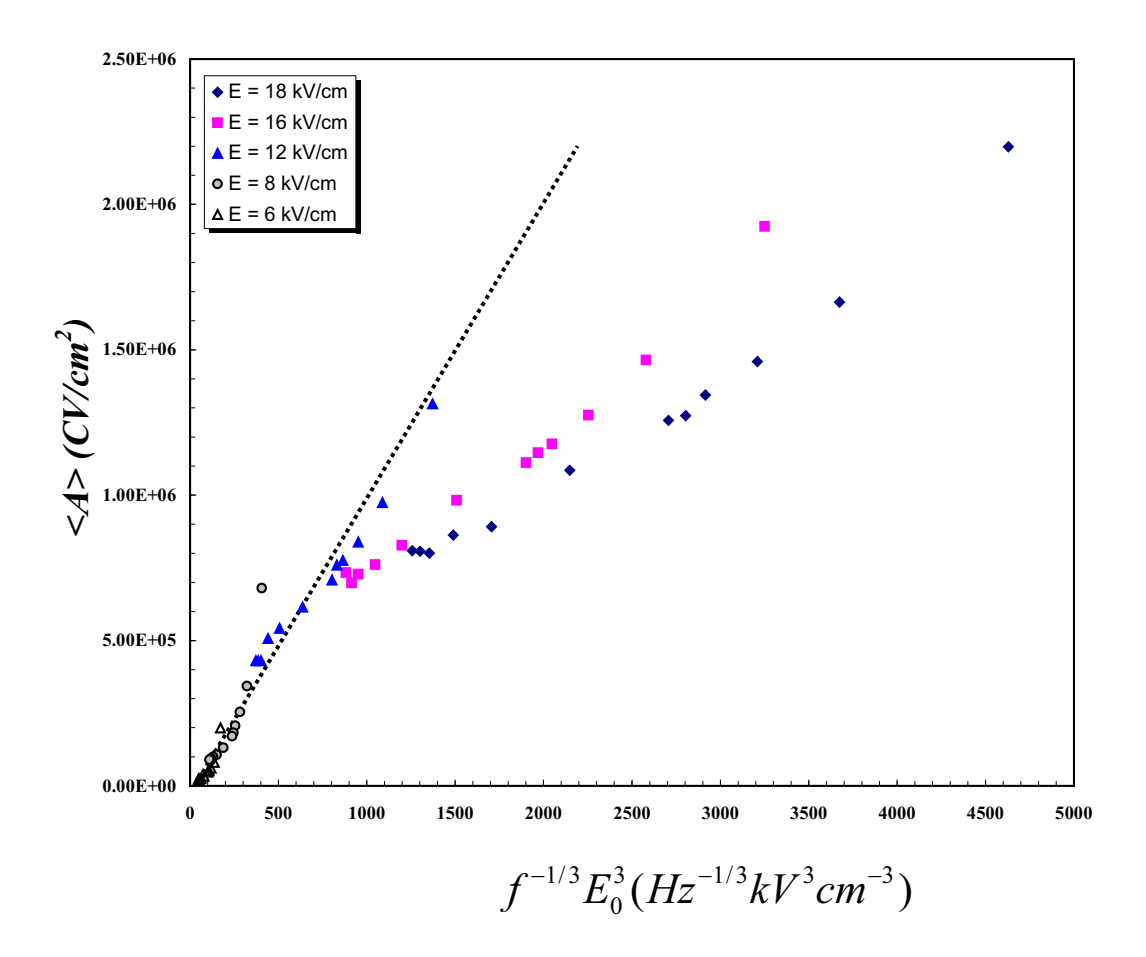
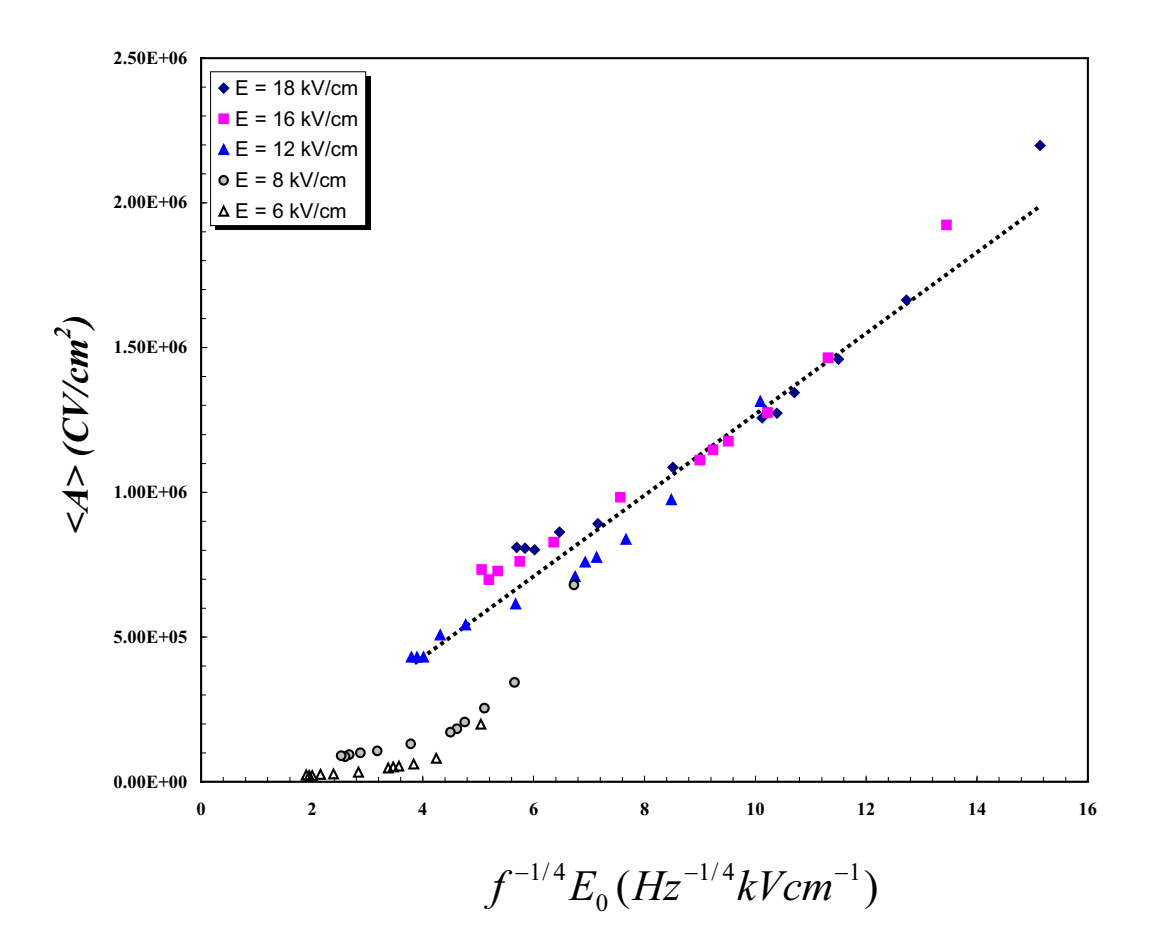


Fig. 3



Stress-Dependent Scaling Behavior of Dynamic Hysteresis in Soft

PZT Bulk Ceramics

Rattikorn Yimnirun, Supattra Wongsaenmai, Supon Ananta,

and Yongyut Laosiritaworn

Department of Physics, Faculty of Science, Chiang Mai University,

Chiang Mai 50200, Thailand

Correspondence Author E-mail: rattikornyimnirun@yahoo.com

PACS numbers: (1) 77. 22. Ch, (2) 77. 84. Dy, (3) 77.80.-e, (4) 77.80.Fm

ABSTRACT

In this study, we performed experiments on soft-PZT bulk ceramics to

investigate the effects of electric field-frequency, electric field-amplitude, and

mechanical stress on the hysteresis area especially the scaling form. The hysteresis

profiles under the effects of relevant parameters were obtained. At stress-free

condition, the investigation found the area scales with frequency and field-amplitude

in power-law form; however, with different set of exponents in comparing to those in

the investigation on thin films structure. This indicates the dimensional dependence of

the exponents. On the other hand, with compressive stresses turning on, the same set of

the exponents with the stress-free condition is found to confirm universality. In

addition, the scaling form of the area to triple parameters; i.e., frequency, field-

amplitude, and stress in a power law form was obtained. The study is therefore

successful in modelling how the hysteresis area decays with increasing stresses at

high-frequencies which provides another step closer in understanding real bulk

ferroelectric materials.

Keywords: Scaling, Stress, Hysteresis, soft PZT

1

1. INTRODUCTION

Lead zirconate titanate (Pb(Zr_{1-x}Ti_x)O₃ or PZT) ceramics have been employed extensively in sensor and actuator applications, as well as smart systems.¹ The most widely studied and used PZT compositions are in the vicinity of the morphotropic phase boundary (MPB) between the tetragonal and rhombohedral ferroelectric phases.^{2,3} However, to meet the requirements for specific applications, PZT ceramics are usually modified with dopants.²⁻⁴ Generally, donor (higher-valency) additives induce "soft" piezoelectric behaviors with higher dielectric and piezoelectric activities suitable for sensor and actuator applications. ¹⁻³ In many of these applications, as well as in more recently developed ferroelectric random access memories (Fe-RAMs), the dynamic hysteresis characteristics have become important consideration. 5,6 In addition to the domain kinetics studies, 7 the dynamic hysteresis, i.e., hysteresis area < A > as a function of the field amplitude E_0 and frequency f, presents a lot of information critical for many ferroelectric applications whose performance is related to the signal amplitude and frequency. 1,6 Theoretical studies have been carried out to understand the dynamic response of hysteresis curves in spin systems.⁸⁻¹¹ In particular, attention is focused on scaling law $< A > \propto f^{\alpha} E_0^{\beta}$ (where α and β are exponents that depend on the dimensionality and symmetry of the system). The theoretical three-dimensional models $((\Phi^2)^2$ and $(\Phi^2)^3$ with O(N) symmetry $(N \rightarrow \infty)$) by Rao et al.⁸ and other investigators^{9,12} proposed two scaling relations applicable to the low-f and high-f limits as follows,

$$< A > \propto f^{1/3} E_0^{2/3}$$
 as $f \to 0$, (1)

$$\langle A \rangle \propto f^{-1} E_0^2 \text{ as } f \to \infty$$
 (2)

Apart from its theoretical importance, since reliable measurement of the hysteresis at ultra-high frequency is still a big challenge, it is technologically helpful to understand the scaling behavior so that the ultra-high frequency of the hysteresis can be predicted. Hence, there has been a great deal of interest in the scaling behavior of the dynamic hysteresis in ferromagnetic and ferroelectric thin films. 10-14 However, only few investigations on ferroelectric and antiferroelectric bulk systems have been reported. 15,16 On a contrary, bulk ferroelectric materials are useful and widely used in many applications. Furthermore, to date, there has been no report on the scaling behavior studies of ferroelectric hysteresis loops of bulk ferroelectric ceramics. Interestingly, some discrepancies between the theoretical predictions and the experimental results have already been reported for ferroelectric thin-films systems. 11,14,17-21 For extended two-dimensional system, the theoretical studies have predicted the scaling relation at high-f limit as in Eq. (2). The experimental investigation, however, on PZT thin films 19 has resulted in a different relation, i.e.,

$$\langle A \rangle \propto f^{-1/3} E_0^3 \text{ as } f \to \infty$$
 (3)

Additionally, another scaling relation has been obtained for the $SrBi_2Ta_9O_4$ thick films, i.e., 17

$$\langle A \rangle \propto f^{-1/3} E_0^2 \quad \text{as} \quad f \to \infty \quad .$$
 (4)

As can be seen, the dimensionality of the structure e.g. thin films in Ref. 19 and thick films in Ref. 17 has a strong effect on the exponent of the scaling relation in Eqs. (3) and (4). It is therefore of great interest to investigate the form of this scaling relation for bulk systems. Hence, one of the aims of this present study is to investigate

the scaling behavior of the dynamic hysteresis of the technically important and commercially available soft PZT bulk ceramic.

More importantly, in many applications the ceramic specimens are often subjected to mechanical loading, either deliberately in the design of the device itself or because the device is used to change shapes as in many smart structure applications or the device is used under environmental stresses. 1-3,6,22 A prior knowledge of how the material properties change under different load conditions is inevitably crucial for proper design of a device and for suitable selection of materials for a specific application. Despite the fact, material constants used in many design calculations are often obtained from a stress-free measuring condition, which in turn may lead to incorrect or inappropriate actuator and transducer designs. It is therefore important to determine the properties of these materials as a function of applied stress. Previous investigations on the stress-dependent electrical properties of many ceramic systems, such as undoped-PZT, PLZT, BT, PMN-PT, PZT-BT, PMN-PZT, 23-32 and PZT and SBT thin films^{33,34} have clearly emphasized the importance of the subject. Many investigations have already revealed interesting results on the electrical properties of the soft PZT ceramics under applied stress. 25,26,30,35 The ferroelectric properties of the soft PZT ceramics have been observed to change significantly with the applied stress. 30,35 However, it is interesting that there have been no report on the influence of the external stress on the scaling behavior of any materials. Therefore, the main aim of this study is to establish the scaling behavior of the dynamic hysteresis responses of soft PZT bulk ceramics under the influence of the external stress.

2. EXPERIMENTS

A commercially available soft PZT ceramic (PKI-552, Piezo Kinetics Inc., USA) was used in this study. Denoted as Navy Type VI, this ceramic is designed for applications that require high electromechanical activity and high dielectric constant. Its properties are (measured by the supplier): longitudinal charge coefficient $d_{33} = 550$ pm/V; planer coupling factor $k_p = 0.63$; dielectric constant (1 kHz) $\varepsilon_r = 3400$; Curie temperature $T_C = 200$ °C; bulk density = 7.6 g/cm³. The disc-shaped samples with diameter of 10 mm and thickness of 1 mm were pre-poled by the supplier.

The dynamic hysteresis (P-E) loops were characterized at room temperature (25 °C) by using a computer controlled modified Sawyer-Tower circuit with f covering from 2 to 100 Hz and E_0 from 0 to 18 kV/cm. The electric field was applied to a sample by a high voltage AC amplifier (Trek, model 610D) with the input sinusoidal signal from a signal generator (Goodwill, model GAG-809). The detailed descriptions of this system are explained elsewhere. 32,35 Effects of the external stress on the dynamic hysteresis were investigated with the compressometer, which was developed for simultaneous applications of the mechanical stress and the electric field.³⁶ The compressometer cell consisting of a cylindrical brass cell with a heavy brass base, a brass ram and a precisely guided loading platform provides true uniaxial stress during mechanical loading. The prepared specimen was carefully placed between the two alumina blocks and the electric field was applied to the specimen via the copper shims attached to the alumina blocks. With this setting, the uniaxial compressive stress was applied parallel to the electric field direction. During the measurements, the specimen was immersed in a silicone oil to prevent high-voltage arcing during electric loading. The compressive stress was supplied by the servohydraulic load frame and the applied stress was monitored with the pressure gauge of the load frame. Measurements were

performed as a function of mechanical stress applied discretely between 0 and 24 MPa. During the measurements, a desired stress was first applied to the sample and then the electric field with varying frequency was applied. The dynamic hysteresis (P-E) loop was then recorded for each applied field and frequency. The measurements reported were for the samples during their first mechanical stress cycle. It should also be noted that the reported ferroelectric parameters were obtained after a total of 10 cycles of the electric field were applied to the sample at each constant stress.

3. RESULTS AND DISCUSSION

From the study, the hysteresis profiles for various frequencies f, field—amplitude E_0 , and stress σ are obtained. Figs. 1(a) and 1(b) show examples of the hysteresis loops at different f but fixed E_0 (18 kV/cm), and at different E_0 but fixed f (100 Hz), respectively, under a stress-free condition. As expected, the dependence of the loop pattern and area A on f and E is remarkable. From Fig. 1(a), where E_0 is fixed, one sees the evolution of the pattern at different f. It is very interesting to observe that as the frequency increases the hysteresis changes from an unsaturated loop with near square shape and rounded at the tips at low frequency (2 Hz) to well saturated loops at higher frequencies. The loop area A, remanent polarization P_r , and coercive field E_r decrease with an increase of frequency. The observation that the A decreases with increasing frequency in this high-P region is ascribed to the delayed response of the spin reversal to the varying external field. It should also be noted that in earlier works by Liu P at P and P are P thin films, the dependence of the P-E loop shape on frequency differed from that of the current work. Since the magnitude of the applied field and the range of the frequency used were significantly

different, the observed difference could be due to the dependence of the loop shape and size on both the field amplitude and frequency, as well as to the different responses to an external field between thin films and bulk ceramics. Figure 1(b) shows the dependence of the hysteresis loop on the amplitude of the electric field. For small fields, the loop does not saturate and appears as an ellipse inclined at an angle to the E axis. An increase in the amplitude of the field E_0 makes the loop larger and increases its angle of inclination. For a given frequency of 100 Hz, as shown in Fig. 1(b), loop area A, remanent polarization P_r , and coercive field E_0 increase with an increase of E_0 until well saturated loop is achieved.

Figure 1(c) displays the hysteresis loops of the soft PZT ceramics under different compressive stress during loading at fixed f of 100 Hz and fixed E_0 of 18 kV/cm. It should first be noticed that the area of the P-E loops decreases steadily with increasing the stress. The P-E loop area indicates the polarization dissipation energy of a ferroelectric material subjected to one full cycle of electric field application.³⁷ This amount of the energy loss is directly related to volume involved in the switching process during the application of electric field.³⁰ When the mechanical stress is applied, more and more ferroelectric domains are constrained by the applied stress and cannot be re-oriented by the electric field so as to participate in the polarization reversal. Consequently, both the saturation and remanent polarizations become lower with increasing the compressive stress. 30,35 The polarization dissipation energy is consequently found to decrease with increasing the applied stress, indicating that the sample volume contributing to polarization reversal decreases with the increasing stress. In the stress-free state, the dissipation energy is $\sim 8.1 \times 10^5$ J/m³; while at 24 MPa, the dissipation energy decreases to 3.8×10^5 J/m³ (< 50% of the stress-free state). Similar observation has also been found in other investigations. ^{23,24,30,38,39}

To investigate the scaling behavior under stress-free condition, we first followed the previous theoretical predictions on the loop—area^{8,9,12} by plotting the data of <*A*> against $f^{-1}E_0^2$. This bases on an assumption that Eq. (2) is applicable, and the frequency range used in this study can be considered as the high frequency region since the loop—area decreases with increasing frequencies. The data are shown in Fig. 2(a) and the dotted line represents a fitting in terms of < *A* $> \propto f^{-1}E_0^2$. Clearly, the theoretically proposed scaling relation in Eq. (2) cannot be directly applied to the data obtained in this study.

On the other hand, earlier experimental work by Liu $et~al.^{19}$ on the scaling behavior of PZT thin films also showed different relation. In those studies, the scaling takes the form of $< A > \propto f^{-1/3} E_0^3$. To check the validity of the relation on the bulk system, i.e., soft PZT ceramic, we plot the data of < A > against $f^{-1/3} E_0^3$. The data are shown in Fig. 2(b) and the dotted line represents a fitting in terms of $< A > \propto f^{-1/3} E_0^3$. Large deviation is also observed in this case. Therefore, this implies that the experimentally obtained scaling relation for the reduced structure i.e. thin films is not applicable to the bulk ceramics.

It is clearly seen that the scaling relations from both the theoretical prediction and the experimental investigation are not applicable for the soft PZT bulk ceramic in this present study. To obtain the suitable scaling relation, one can fit the data with $\langle A \rangle \propto f^m E_0^n$ where m and n are exponents to be determined directly from the experimental data. By plotting $\langle A \rangle$ against f at fixed E_0 , one obtains the exponent m. On the other hand, the exponent n can be obtained from plotting $\langle A \rangle$ against E_0 at fixed f. It should also be noted that there is more deviation from the minor loops without saturation at small field amplitudes, and these data were excluded from the

fitting reported. It can be seen in Figs. 3(a) and 3(b) that the suitable exponent m for the frequency component has the value of -0.25 (within the limit of experimental errors), while the hysteresis area <A> is found to increase linearly with the applied field amplitude E_0 , hence the exponent n should take the value of 1. Therefore, as plotted in Fig. 4, it is revealed that the data obtained under stress-free condition can be much better fitted (with $R^2 = 0.97$), within the measured uncertainty, by

$$< A > \propto f^{-0.25} E_0$$
 (5)

Therefore, Eq. (5) is identified as the suitable scaling relation for the soft PZT bulk ceramic under the stress-free condition. The scaling relation obtained indicates that area $\langle A \rangle$ decays more slowly with f and grows more slowly with E than the theoretical prediction, Eq. (2). It is also interesting to see that the area $\langle A \rangle$ also decays slightly slower with f, but grows much more slowly with E than the PZT thin films, Eq. (3). There have also been reports on the scaling studies on other bulk systems, such as ferroelectric single crystals TGS¹⁵ and antiferroelectric bulk system BP_{0.9}A_{0.1}¹⁶, with very different scaling relations as compared to that of this current study on bulk ceramic. Though these are bulk systems, these are still different types of materials, as compared to the ceramic studied here, thus their scaling behaviors cannot be directly compared.

An explanation for the difference may come from the spin-interaction terms as considered in the $(\Phi^2)^2$ and $(\Phi^2)^3$ models, in which the spin-flip just has one contribution, i.e. spin-reversal.^{8,9} This requires overcoming high energy barrier. Potts model used by Liu *et al.*¹⁹ also has the spin orientation in various domains in directions not anti-parallel to the direction of E, hence requires lower energy barrier for spin-flip to occur, which results in a higher exponent of 3 in the E_0 term, as

compared to the exponent of 2 in the theoretical models. However, in ceramics, there are influences of many depolarizing effects, arisen from domain walls, grain boundaries, space charges, immobile defects *etc.*, which may retard the external field. Consequently, the energy barrier is very much higher, which leads to slower spin-flip kinetics. Therefore, a low exponent for the E_0 term is expected from the ceramics rather than the $(\Phi^2)^2$, $(\Phi^2)^3$ and Potts models, and thin films. This may be the case, as also reported in Ref. 18, why the decay of the area A with frequency f and field amplitude E_0 is much smaller than those from theoretical prediction i.e. $A > \infty f^{-1/3}E_0$ instead of $A > \infty f^{-1}E_0^2$.

In addition, the f-term shows an exponent of -0.25, smaller in absolute value than that of PZT thin-films (exponent is -1/3). To explain the difference, not only the contribution from the domain switching and ionic-type in thin films, one may need to consider the additional contributions to hysteresis properties from space charges on grain boundaries, induced electric-field from interface layers, immobile defects, etc. Since our system is a bulk-ceramic type; therefore, these depolarizing effects, acting as a buffer to spin-reversal mechanism, will be stronger than those in thin films structure. As a result, the hysteresis area must show a relatively weaker dependence on f than that observed in thin films. More importantly, this study shows the difference in experimentally observed scaling behavior between thin films and bulk ceramics, suggesting the different universality class between them.

Moreover, as evident in Figs. 1(c) and 3(c), at any given frequencies the hysteresis area $\langle A \rangle$ is found to decrease steadily with increasing the applied stress. Therefore, instead of including only the field amplitude E_0 and the frequency term f, the scaling relation should also include the stress (σ) term, i.e.

$$\langle A \rangle \propto f^m E_0^n \sigma^p$$
 (6)

However, due to increasing number of exponents, to simplify the problem, we assume the validity of the scaling form $\langle A \rangle(\sigma) \propto f^{-0.25}E_0$ for all applied stresses. Consequently, the area $\langle A \rangle$ for each stress is plotted against $f^{-0.25}E_0$, as shown in Fig. 5. As can be seen form the least–square linear fits, reasonably good linear relations can be found. As a result, the condition of universality having m=-0.25 and n=1 in soft–PZT bulk ceramic systems is confirmed whereas the proportional constant in Eq. (6) may still be a function of σ . Therefore, to investigate the σ -dependence of the area $\langle A \rangle$ in details we generalize Eq. (6) by writing,

$$\langle A \rangle = G(\sigma) f^{-1/4} E_0 + F(\sigma), \tag{7}$$

where both $G(\sigma)$ and $F(\sigma)$ are assumed to be a function of σ representing slope—function and y—intercept—function for a 'linear—relation' in Eq. (7), and their values are presented via linear—fit functions in Fig. 5. Next, to obtain the scaling form as indicating in Eq. (6), we assumed the slope—function G(s) to take a form of power—law function, i.e.

$$G(\sigma) = a + b\sigma^c. \tag{8}$$

However, for the y-intercept-function F(s), the scattering data in F(s) do not follow a trivial power-law form. Instead, the best function that suits F(s) is found to take a polynomial degree-3 function, i.e.

$$F(\sigma) = a_0 + a_1 \sigma + a_2 \sigma^2 + a_3 \sigma^3.$$
 (9)

Next, performing a non-linear fit for G_G gives $a=2.73\times10^6\pm0.42\times10^6$, $b=-0.38\times10^6\pm0.30\times10^6$, and $c=0.44\pm0.17$ with $R^2\approx0.994$. On the other hand, a degree-3 polynomial fit for F_G gives $a_0=-0.46\times10^6\pm0.11\times10^6$, $a_1=97.30\times10^3\pm45.59\times10^3$, $a_2=-9.52\times10^3\pm4.76\times10^3$, a n d $a_3=0.21\times10^3\pm0.13\times10^3$ with $R^2\approx0.878$. The fitting formalisms to relevant parameters for the slope-function Eq. (8) and the *y*-intercept-function Eq. (9) are presented in Fig. 6.

As a result, from Eqs. (7) to (9), it is therefore possible to write,

$$\frac{\langle A \rangle - F(\sigma)}{G(\sigma)} = f^{-0.25} E_0, \tag{10}$$

and by plotting this scaling area $\frac{\langle A \rangle - F(\sigma)}{G(\sigma)}$ against $f^{-0.25}E_0$ all the data should collapse onto a single linear line having a y-intercept at zero. The data-collapsing of the scaling area from all f, E_0 , and σ was found to confirm Eq. (10) as evident in Fig. 7.

On the other hand, it is of interest if we are allowed to have the scaling of $\langle A \rangle$ in a form given by Eq. (6). Therefore, by discarding minor loops which usually occur at very low E_0 , $F(\sigma) \equiv \langle A \rangle (E_0 \to 0)$ will be small in comparing to $\langle A \rangle$ and can be discarded in Eq. (10) at some intermediately high fields. Consequently, we may write $\langle A \rangle \propto (a + b\sigma^c) f^{-0.25} E_0$ and by substituting the fitted parameters, it is found that

$$\langle A \rangle - \langle A_{\sigma=0} \rangle = \langle A - A_{\sigma=0} \rangle \propto f^{-0.25} E_0 \sigma^{0.44},$$
 (11)

where $\langle A_{s=0} \rangle$ refers to stress–free hysteresis area which will be a dominant term for zero stress. Note that from the appearance of stress s, $\langle A-A_{s=0} \rangle$, referring to the difference in energy dissipation between under–stress and stress–free condition, increases with increasing stress suggesting a decay of $\langle A \rangle$ with s at a rate of s 0.44 as observed in experiments. As a result, from our studies, it may be concluded that in bulk ceramics, the difference of the hysteresis area between under–stress and stress–free condition scales with frequency, field–amplitude and stress via exponents m=-0.25, n=1, and p=0.44. However, at a particular fixed stress, Eq. (11) yields Eq. (5) which is the original form for how the area scales with the frequency and the field–amplitude.

4. CONCLUSIONS

In this study, we investigated the hysteresis properties of the soft–PZT bulk ceramics under the effect of mechanical stress at various frequencies and field–amplitudes of the external applied electric field. The effect of the stress, frequency, and amplitude on the hysteresis loop is notable in a good agreement with previous investigations. Considering the scaling law for the loop–area, at zero stress, the investigation found the area scales with frequency and the field–amplitude in a power law function. However, the exponents to the scaling in this bulk ceramic system do not match with previous investigation on thin films structure indicating that the exponent is dimensionally dependent. On the other hand, with inserting the uniaxial stress, the same set of exponents to frequency and field–amplitude in stress–free condition is

found which confirms the condition of universality in bulk system. Furthermore, the difference of the energy dissipation between the under–stress and stress–free condition is found to scale with $f^{-0.25}E_{0^{s}}^{-0.44}$. As a result, the study provides a detailed understanding of how the energy dissipation of the hysteresis properties behaves in response to various conditions especially the mechanical stress which is the novel point in this study. Therefore, the study provides another step closer in modeling real materials which may be used to boost up the technological development to obtain highly functional applications made from ferroelectric materials.

ACKNOWLEDGMENTS

Financial supports from the Commission on Higher Education (CHE), Thailand Research Fund (TRF), and Faculty of Science and Graduate School of Chiang Mai University are gratefully acknowledged.

References

- ¹K. Uchino, Ferroelectric Devices (Marcel Dekker, New York, 2000).
- ²B. Jaffe, W. R. Cook, and H. Jaffe, *Piezoelectric Ceramics* (Academic Press, New York, 1971).
- ³Y.H. Xu, Ferroelectric Materials and Their Applications (North Holland, Los Angeles, 1991).
- ⁴F. Kulcsar, J. Am. Ceram. Soc. **42**, 49 (1959).
- ⁵J.F. Scott, Ferroelectr. Rev. **1**, 1 (1998).
- ⁶K. Uchino, *Piezoelectric Actuators and Ultrasonic Motors* (Kluwer Academic, Boston, 1997).
- ⁷J.D. Gunton, M. San Miguel, and P.S. Sahmi, in *Phase Transitions and Critical Phenomena*, edited by C. Domb and J.L. Lebowitz (Academic, London, 1983), Vol 8, p. 267.
- ⁸M. Rao, H.R. Krishnamurthy, and R. Pandit, Phys. Rev. B 42, 856 (1990).
- ⁹M. Acharyya and B.K. Chakrabarti, Phys. Rev. B **52**, 6560 (1995).
- ¹⁰J.-M. Liu, H.L.W. Chan, C.L. Choy, and C.K. Ong, Phys. Rev. B **65**, 014416 (2001).
- ¹¹J.-M. Liu, H.L.W. Chan, C.L. Choy, Y.Y. Zhu, S.N. Zhu, Z.G. Liu, and N.B. Ming, Appl. Phys. Lett. **79**, 236 (2001).
- ¹² M. Rao and R. Pandit, Phys. Rev. B **43**, 3373 (1991).
- ¹³Q. Jiang, H.N. Yang, and G.C. Wang, Phys. Rev. B **52**, 14911 (1995).
- ¹⁴B. Pan, H. Yu, D. Wu, X.H. Zhou, and J.-M. Liu, Appl. Phys. Lett. **83**, 1406 (2003).
- ¹⁵S. Hashimoto, H. Orihara, and Y. Ishibashi, J. Phys. Soc. Jpn. **63**, 1601 (1994).
- ¹⁶Y.-H. Kim and J.-J. Kim, Phys. Rev. B. **55**, R11933 (1997).
- ¹⁷J.-H. Park, C.-S. Kim, B.-C. Choi, B.K. Moon, J.H. Jeong, and I.W. Kim, Appl. Phys. Lett. **83**, 536 (2003).
- ¹⁸J.-M. Liu, H.P. Li, C.K. Ong, and L.C. Lim, J. Appl. Phys. **86**, 5198 (1999).
- ¹⁹J.-M. Liu, H.L.W. Chan, and C.L. Choy, Mater. Lett. **52**, 213 (2002).
- ²⁰J.-M Liu, B. Pan, K.F. Wang, and H. Yu, Ceram. Inter. **30**, 1471 (2004)
- ²¹ J.-M. Liu, H. Yu, B. Pan, and X.Y. Chen, Mater. Sci. Eng. **B118**, 2 (2005).
- ²²L.E. Cross, Mater. Chem. Phys. **43**, 108 (1996).
- ²³I.J. Fritz, J. Appl. Phys. **49**, 4922 (1978).
- ²⁴C.S. Lynch, Acta Mater. **44**, 4137 (1996).

- ²⁵Q.M. Zhang, J. Zhao, K. Uchino, and J. Zheng, J. Mater. Res. **12**, 226 (1997).
- ²⁶J. Zhao, A.E. Glazounov, and Q.M. Zhang, Appl. Phys. Lett. **74**, 436 (1999).
- ²⁷D. Viehland and J. Powers, J. Appl. Phys. **89**, 1820 (2001).
- ²⁸R. Yimnirun, S. Ananta, E. Meechoowas, and S. Wongsaenmai, J. Phys. D: Appl. Phys. **36**, 1615 (2003).
- ²⁹D. Viehland, J.F. Li, E. McLaughlin, J. Powers, R. Janus, and H. Robinson, J. Appl. Phys. **95**, 1969 (2004).
- ³⁰D.Zhou, M. Kamlah, and D. Munz, J. Euro. Ceram. Soc. **25**, 425 (2005).
- ³¹D. Viehland, F. Tito, E. McLaughlin, H. Robinson, R. Janus, L. Ewart, and J. Powers, J. Appl. Phys. **90**, 1496 (2001).
- ³²R. Yimnirun, S. Ananta, A. Ngamjarurojana, and S. Wongsaenmai, Appl. Phys. A-Mater. **81**, 1227 (2005).
- ³³T. Kumazawa, Y. Kumagai, H. Miura, M. Kitano, and K. Kushida, Appl. Phys. Lett. **72**, 608 (1998).
- ³⁴X. Lu, J. Zhu, X. Li, Z. Zhang, X. Zhu, D. Wu, F. Yan, Y. Ding, and Y. Wang, Appl. Phys. Lett. **76**, 3103 (2000).
- ³⁵R. Yimnirun, Y. Laosiritaworn, and S. Wongsaenmai, J. Phys. D: Appl. Phys. **39**, 759 (2006).
- ³⁶R. Yimnirun, P.J. Moses, R.J. Meyer, and R.E. Newnham, Rev. Sci. Instrum. **74**, 3429 (2003).
- ³⁷M.E. Lines and A.M. Glass, *Principles and Applications of Ferroelectrics and Related Materials* (Clarendon Press, Oxford, 1977).
- ³⁸D. Fang and C. Li, J. Mater. Sci. **34**, 4001 (1999).
- ³⁹O. Guillon, P. Delobelle, F. Thiebaud, V. Walter, and D. Perreux, Ferroelectrics. **308**, 95 (2004).
- ⁴⁰D. Bolten, U. Böttger, and R. Waser, Appl. Phys. Lett. **84**, 2379 (2004).
- ⁴¹D. Bolten, U. Böttger, and R. Waser, Jpn. J. Appl. Phys. **41**, 7202 (2002).

List of Figure Captions

- Fig. 1 Hysteresis loops for soft PZT ceramic (a) at various $f(E_0 = 18 \text{ kV/cm})$ and $\sigma = 0 \text{ MPa}$, (b) at various E_0 (f = 100 Hz and $\sigma = 0 \text{ MPa}$), and (c) at various σ (f = 100 Hz and $E_0 = 18 \text{ kV/cm}$).
- **Fig. 2** Scaling of hysteresis area <A> against (a) $f^{-1}E_0^2$ and (b) $f^{-1/3}E_0^3$ for soft PZT ceramic under stress-free condition.
- **Fig. 3** Hysteresis area <A> against (a) f (at various E_0 and $\sigma=0$ MPa), (b) E_0 (various f and $\sigma=0$ MPa), and (c) σ (various f and $E_0=18$ kV/cm) for soft PZT ceramic.
- **Fig. 4** Scaling of hysteresis area <A> against $f^{-0.25}E_0$ for soft PZT ceramic under stress-free condition.
- **Fig. 5** Scaling of hysteresis area <A> against $f^{-0.25}E_0$ for soft PZT ceramic at various compressive stresses.
- Fig. 6 Non-linear fits to the slope-function G(s) and the y-intercept-function F(s) of the hysteresis area A> under the effect of compressive stress A> under the effect of compressive stres
- Fig. 7 The collapse of the scaling area $\frac{\langle A \rangle}{G(s)}$ against $f^{-0.25}E_0$ on a same linear-line (with small fluctuation) for soft PZT ceramic.

Fig. 1 (a)

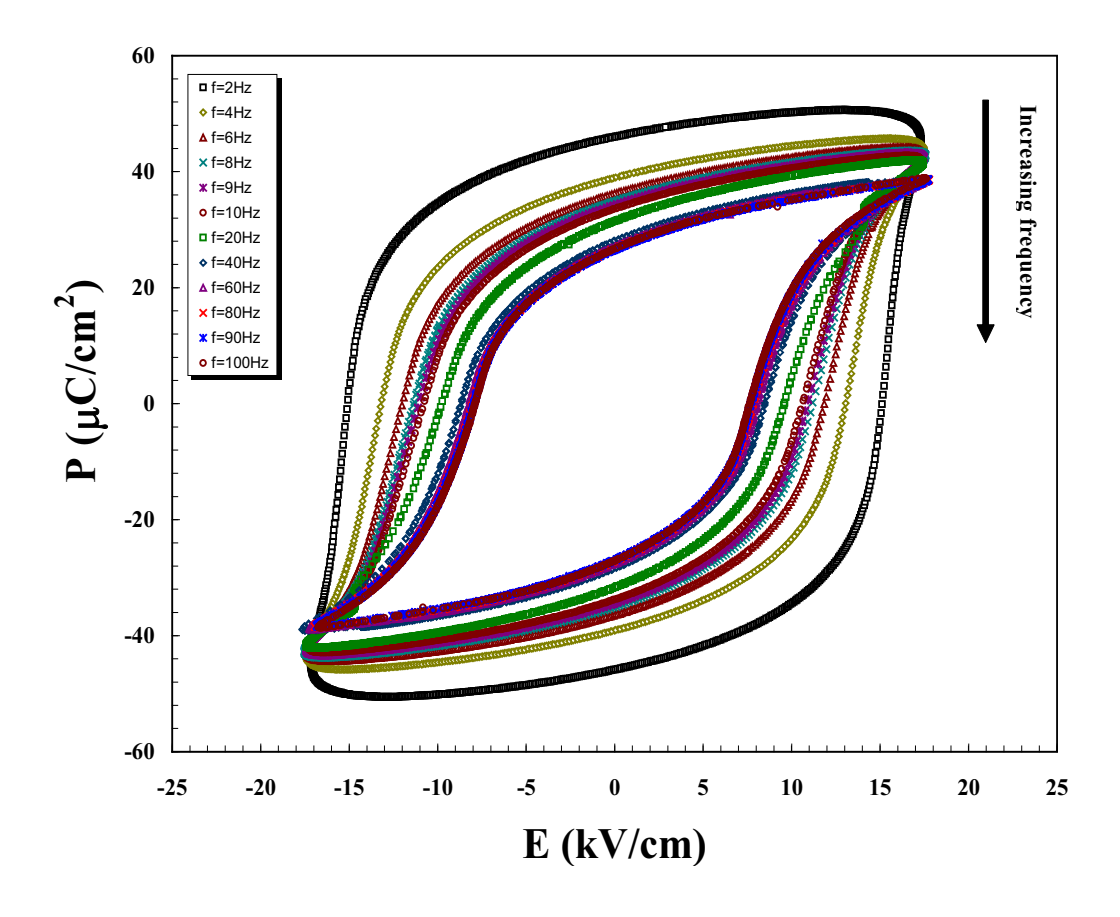


Fig. 1 (b)

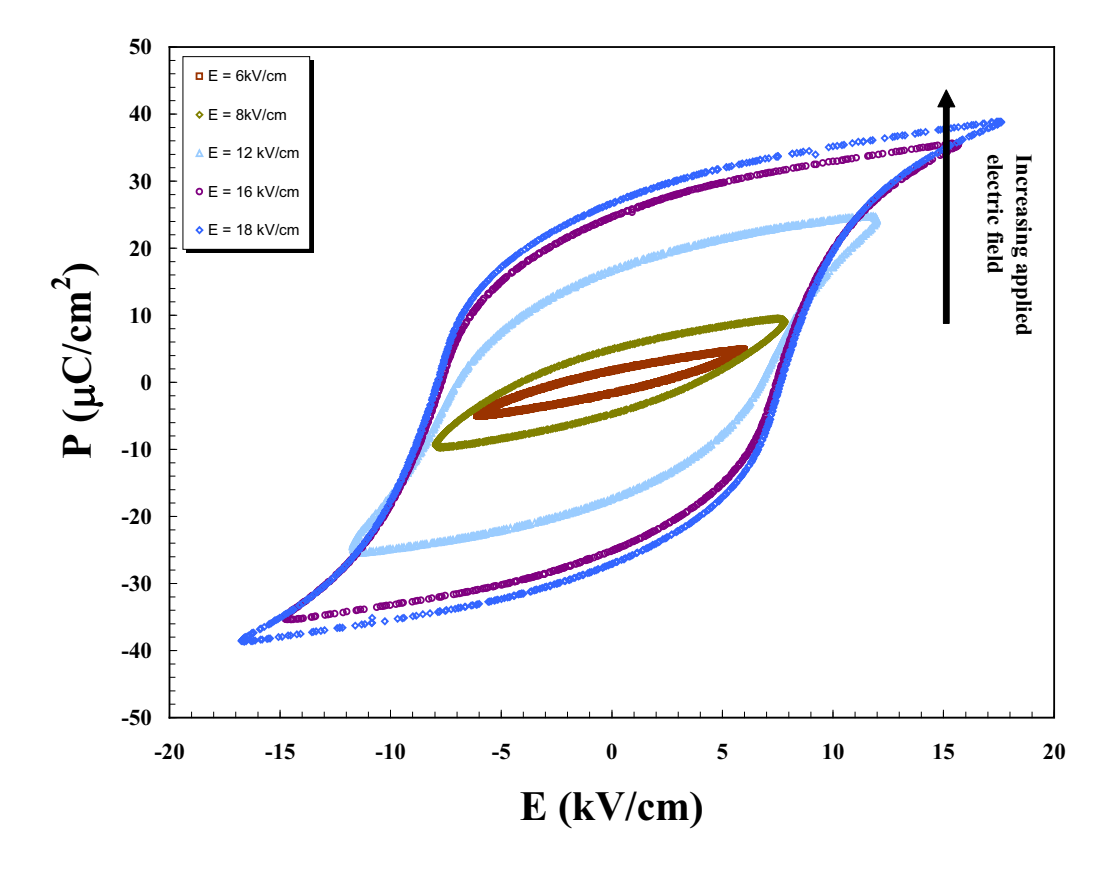


Fig. 1(c)

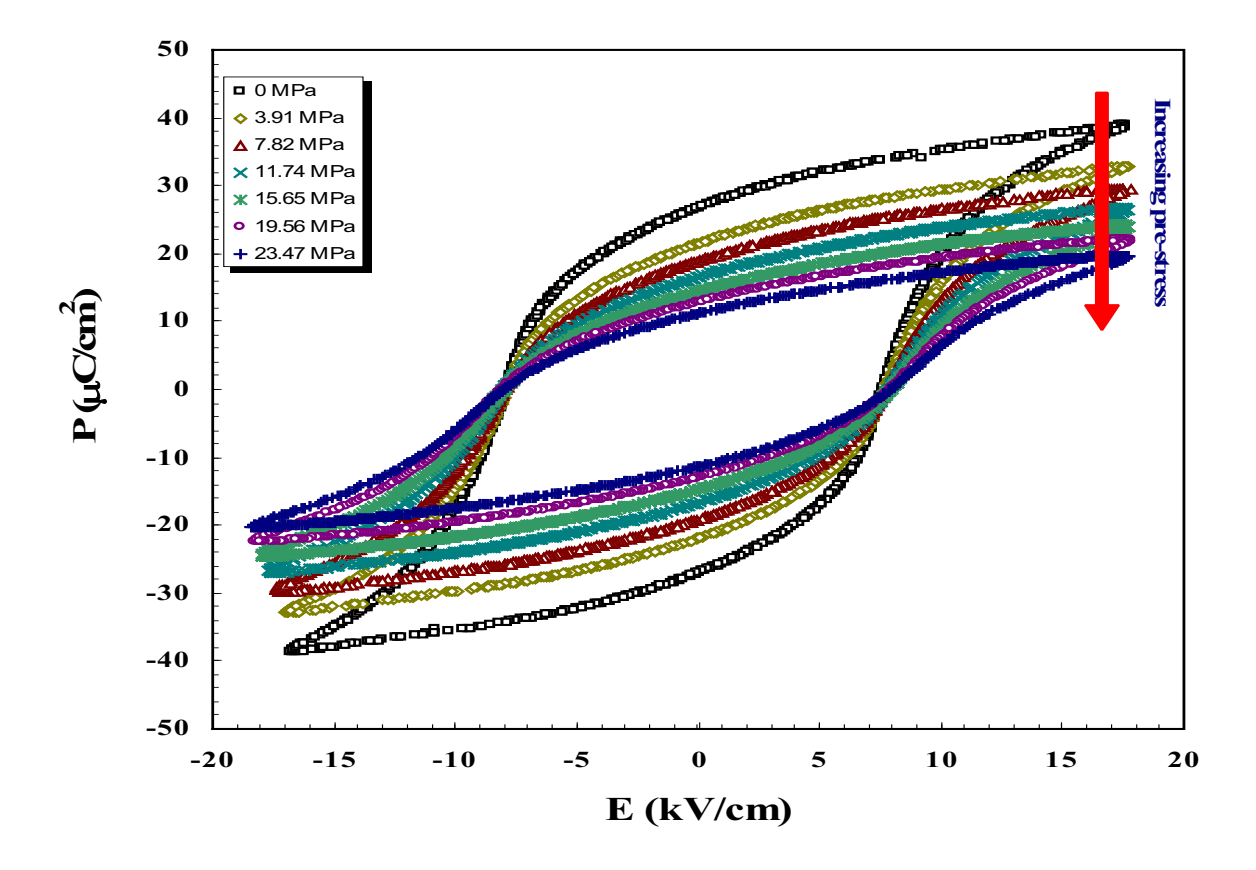


Fig. 2(a)

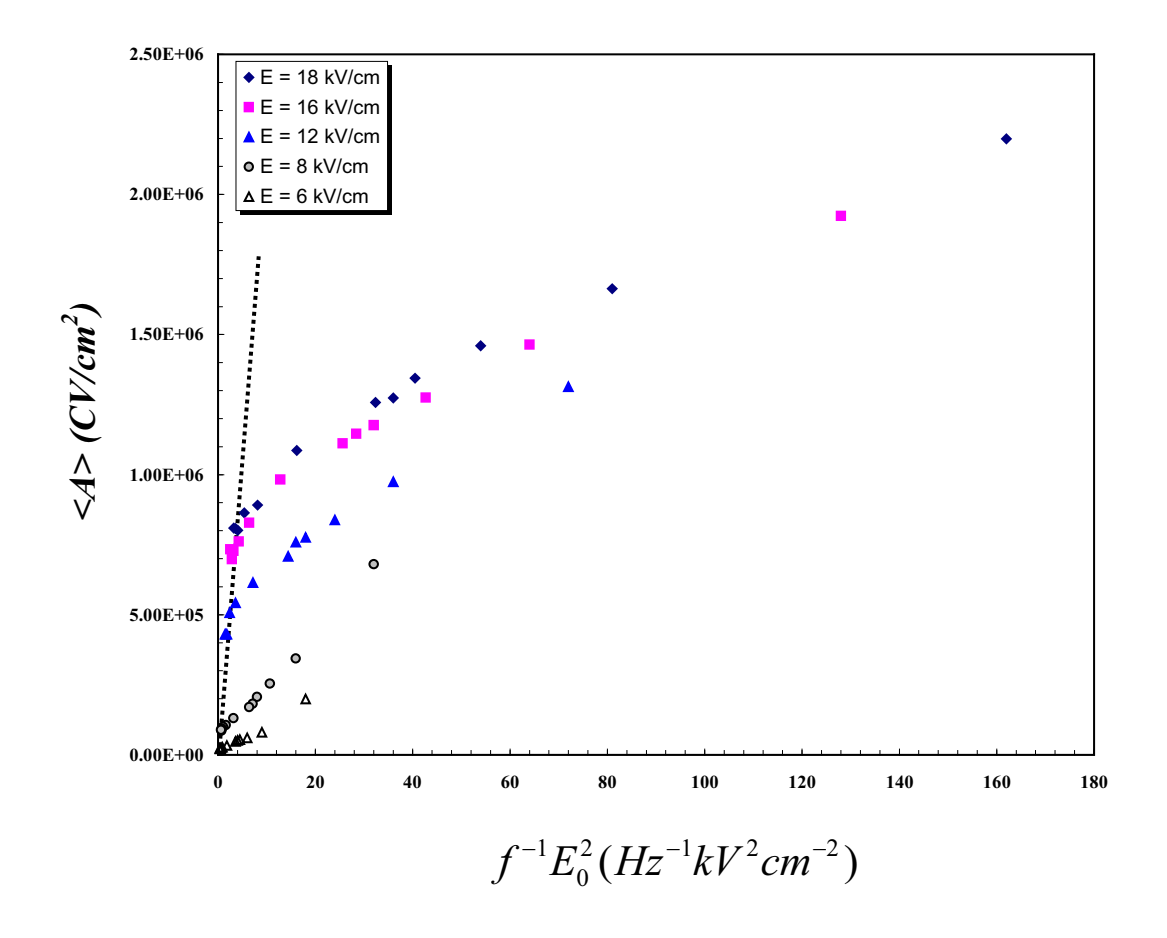


Fig. 2(b)

